Microfluidic Bubble Logic

Manu Prakash
Massachusetts Institute of Technology

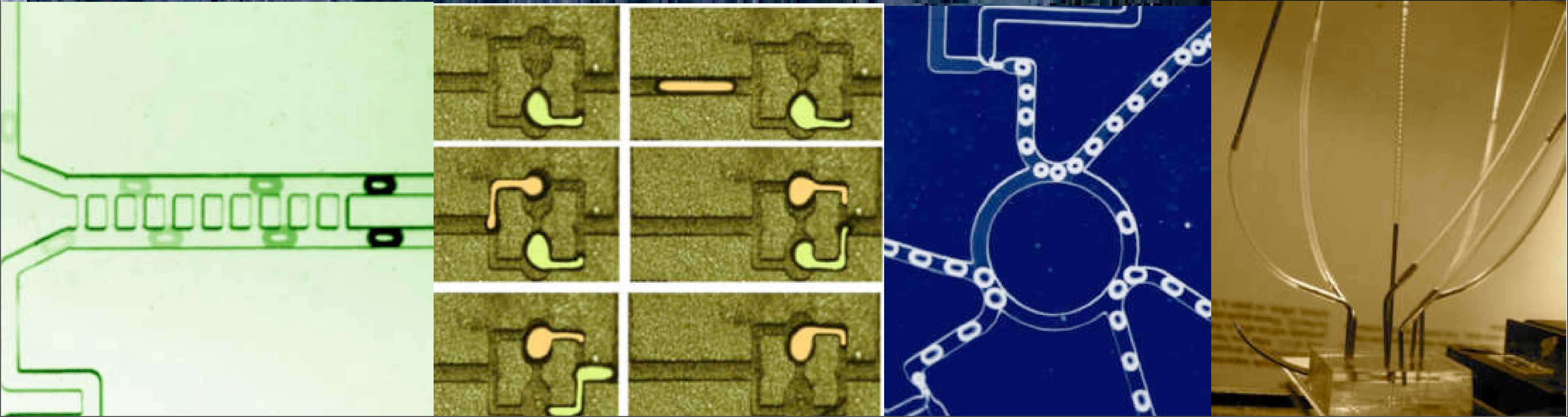

Future of materials (chemical/biological) processing

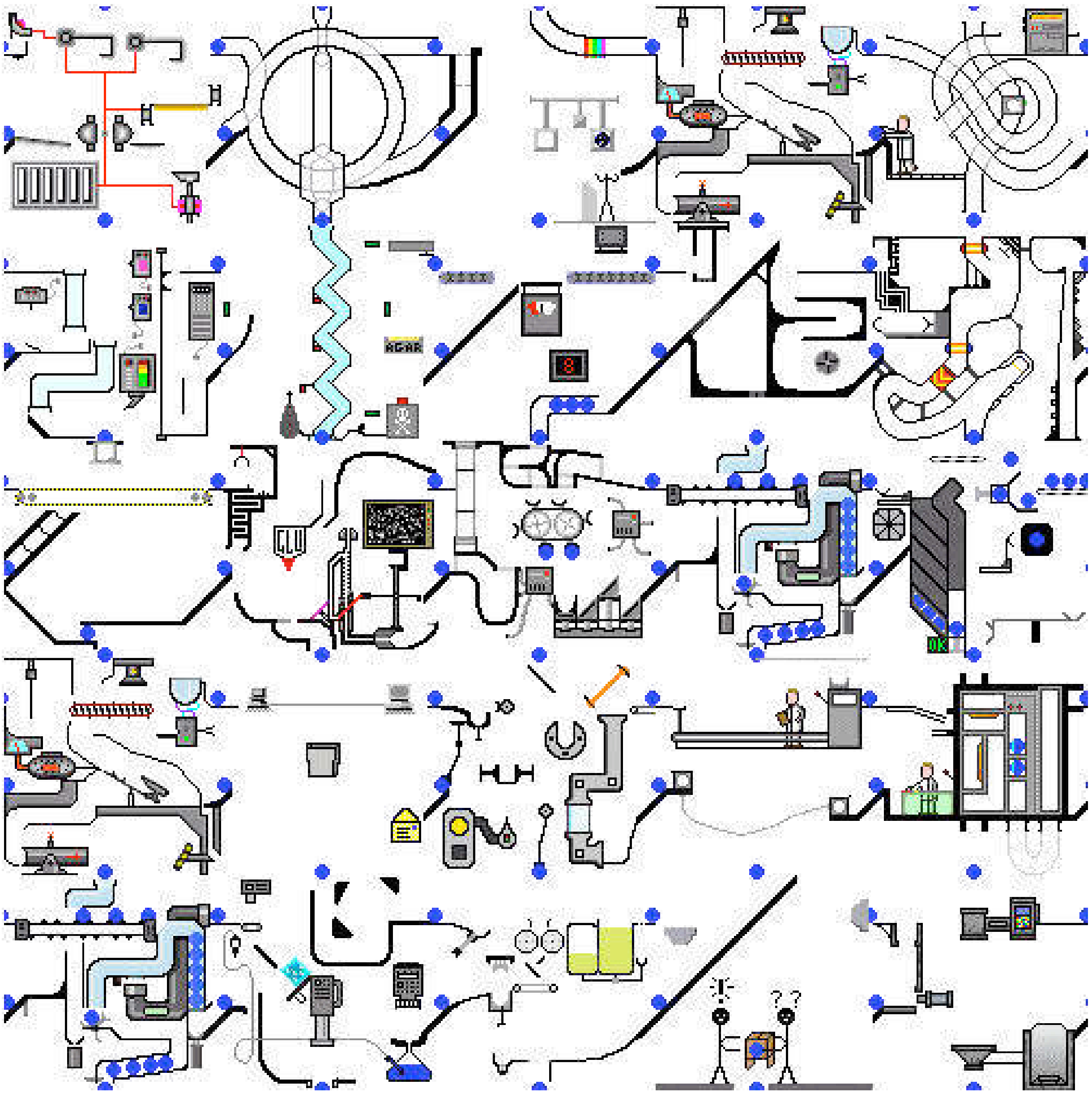

Bubble logic
Capillary ratchet
Micro-slot detector

Information is Physical

"Information is inevitably tied to a physical degree of freedom through a charge, a spin, a hole in punch card or chalk marks on a blackboard"

Rolf Landauer, 93

↓

Bits are Atoms

↓

$\boxed{\text{Information processing => Material processing}}$

Drops and Bubbles

1737

Young man blowing bubbles
Oil on canvas 61 x 63 cm
Metropolitan Museum of Art, New York

2007

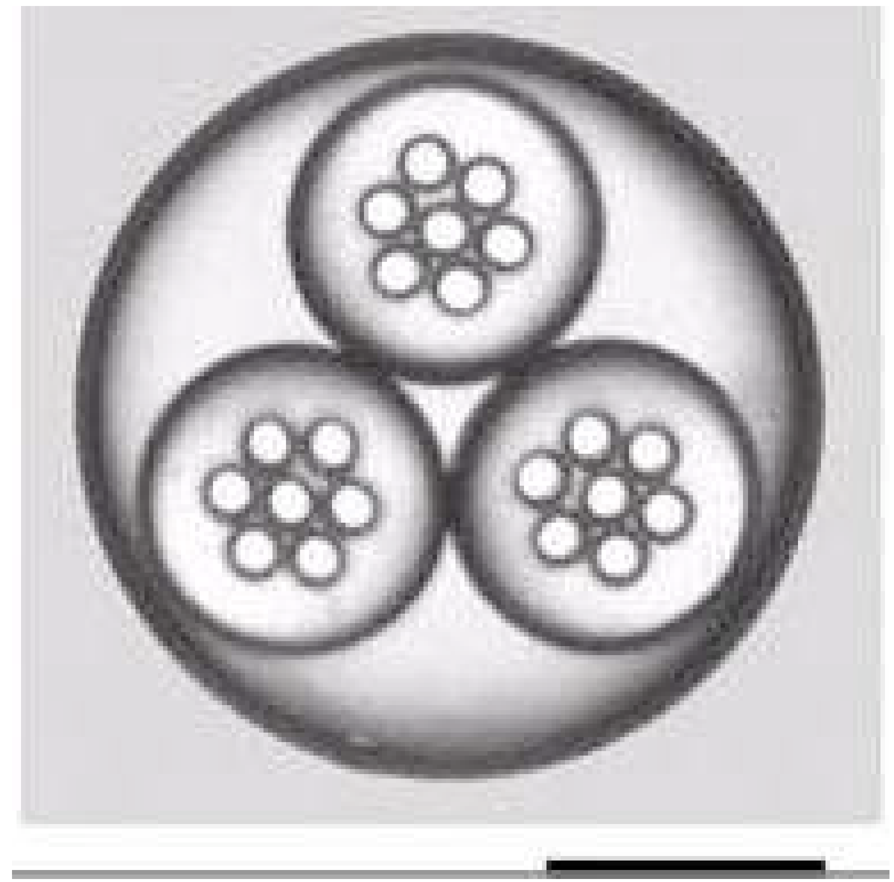

Weitz Group, Harvard

Trapping

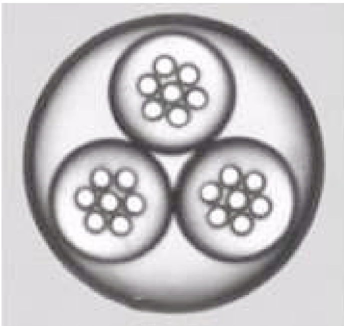

Weitz 2007 (unpublished)

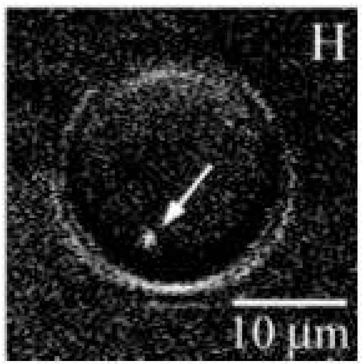

D. Chiu, Anal. Chem 2005

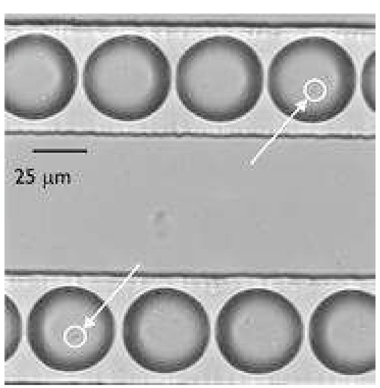

Huebner et al. ChemComm Jan 2007

Recations

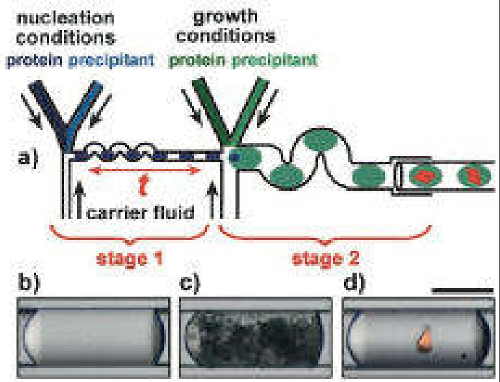

Multi-step protein (thaumatin) crystallization Ismagilov, Angew. Chem. 2006

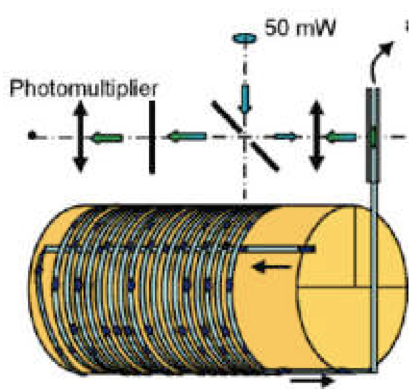

PCR in a drop (Chabert, Nov. 06)

Optimization/ Mixing

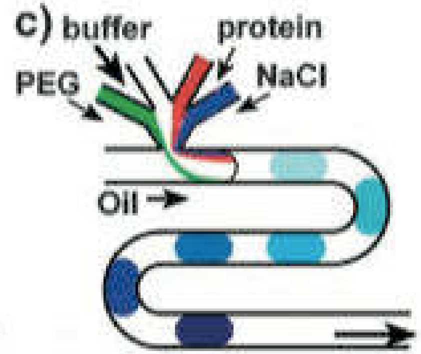

Gradient screening for crystallization conditions Ismagilov,04

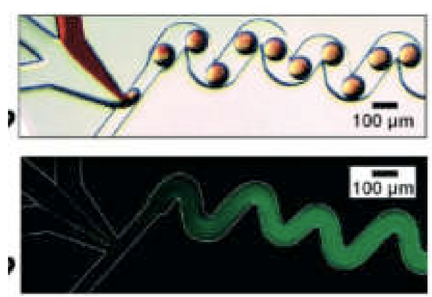

Milli-second time scale mixing

Storage

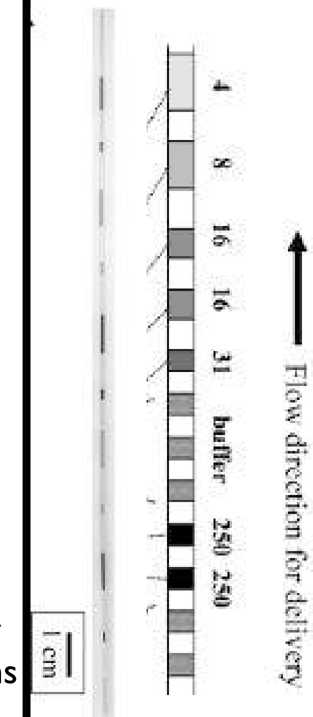

Whitesides 05

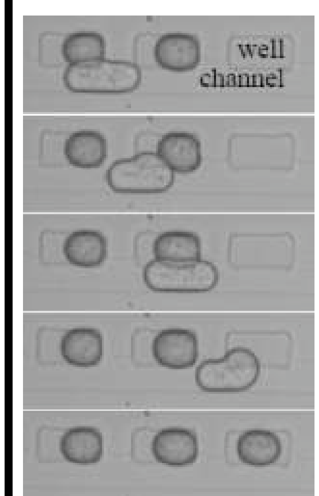

Fraden 06

Detection

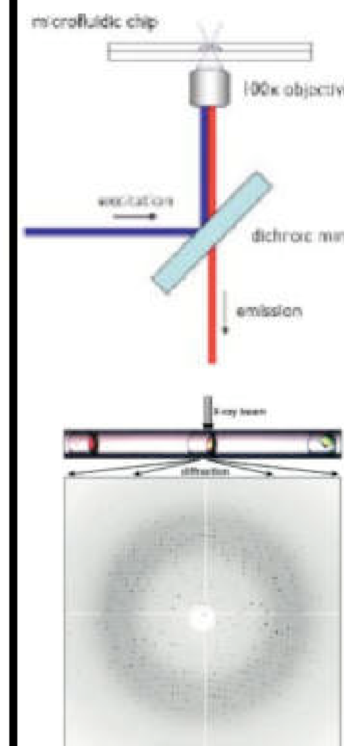

Ismagilov 2006

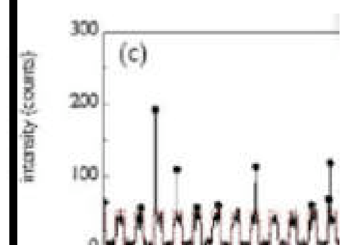

Huebner ChemComm07

Control Strategies

portability
scaling

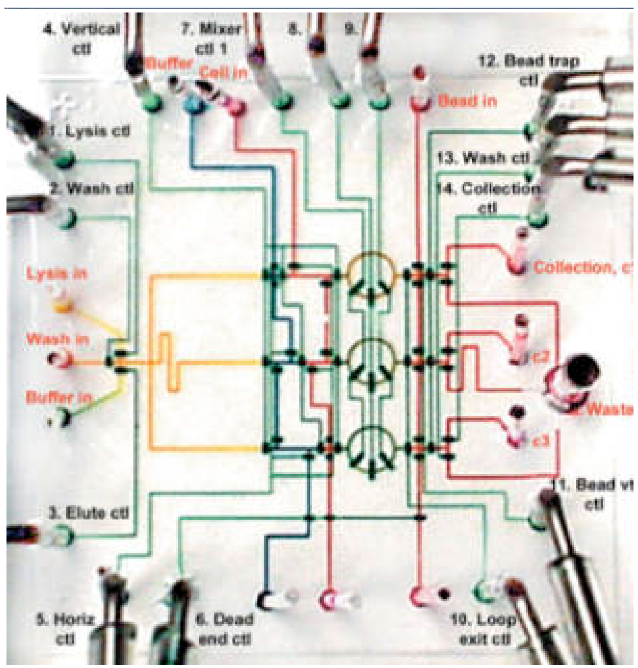

Fluidigm

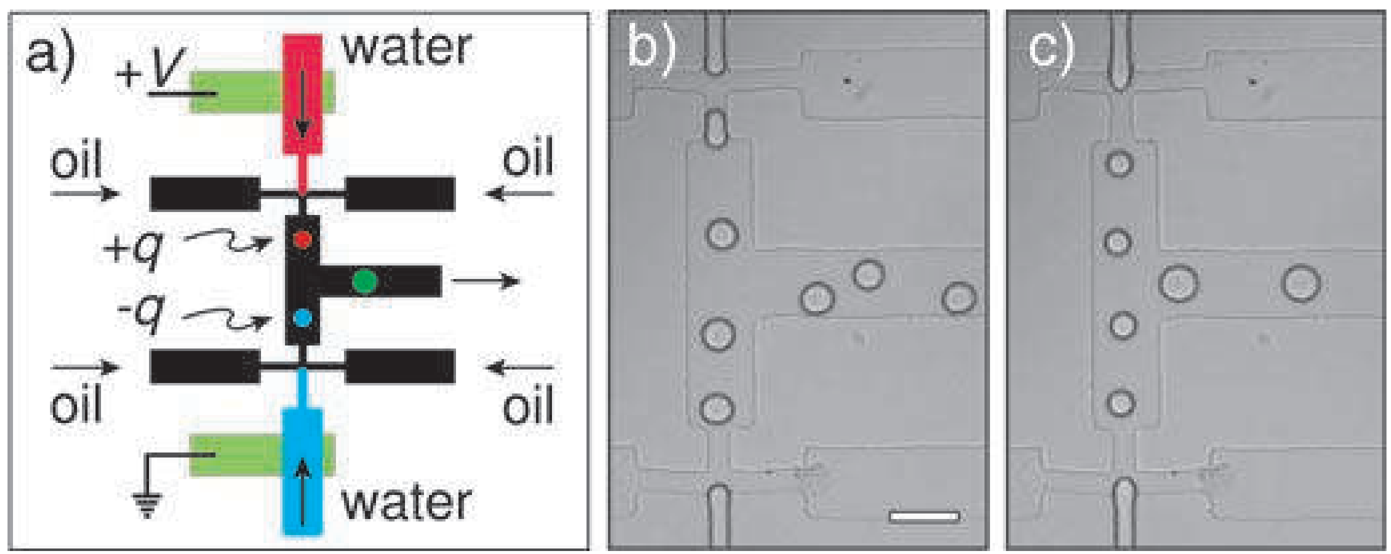

RainDance
Technologies

Fluidic Computing

1965

2003

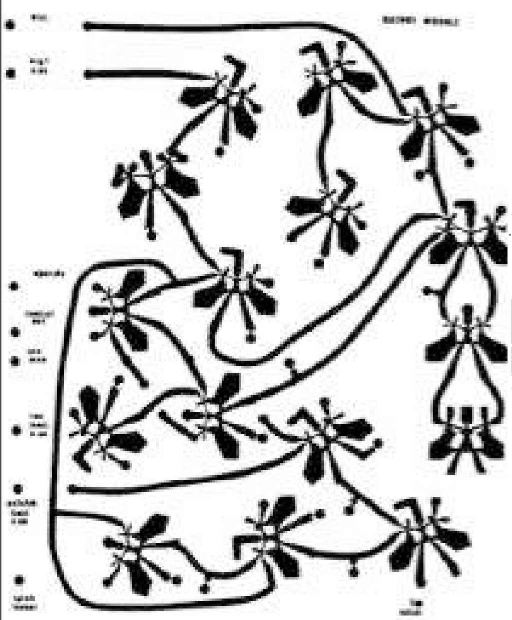

Figure 11. Demonstration Fluidic Computer in Operation

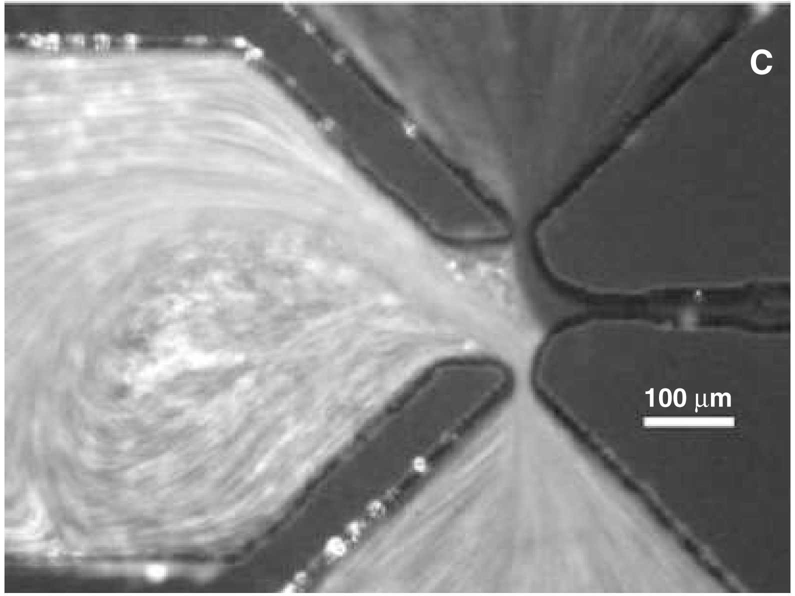

Wall attachment - Coanda effect
Jet interaction - Inertial effects

large Re number systems

[Humphery et al. Fluidics 1965]

Requires non-newtonian fluids for operation

[Quake et al. Science 2003]

Bubble Logic
On-chip process control

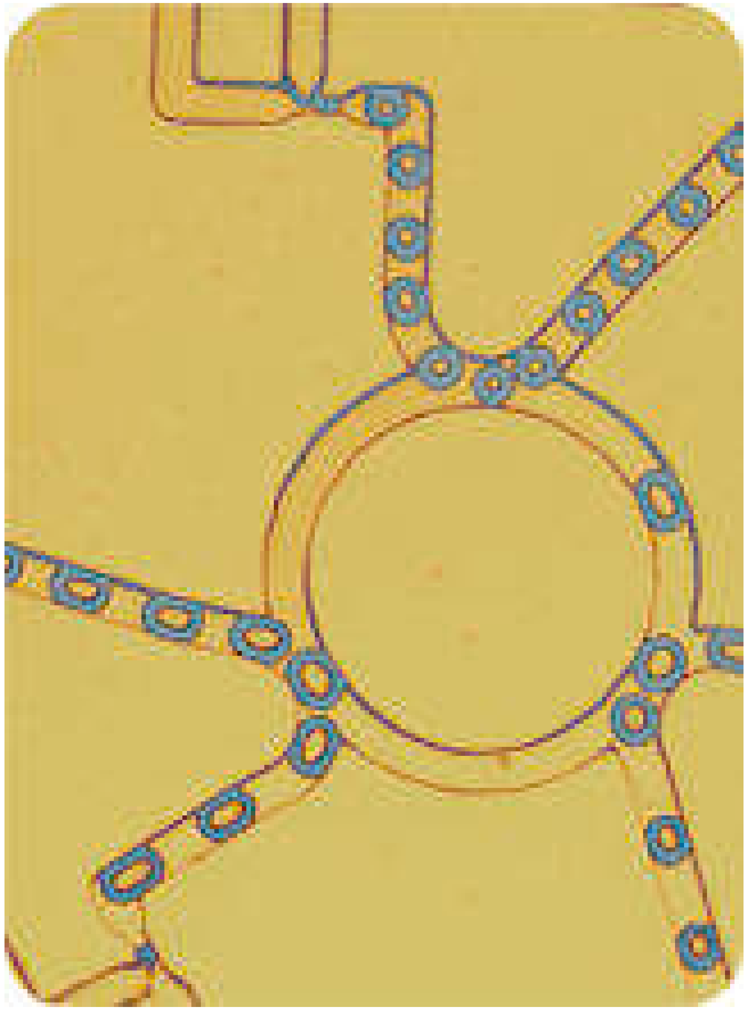

Image credit : F. Frenkel, M. Prakash

- A bubble is a bit of information, but can also carry a material payload
- Integrating chemistry and computation

[Prakash, Gershenfeld; Science Vol. 315 2007]

Programmed generation of bubbles

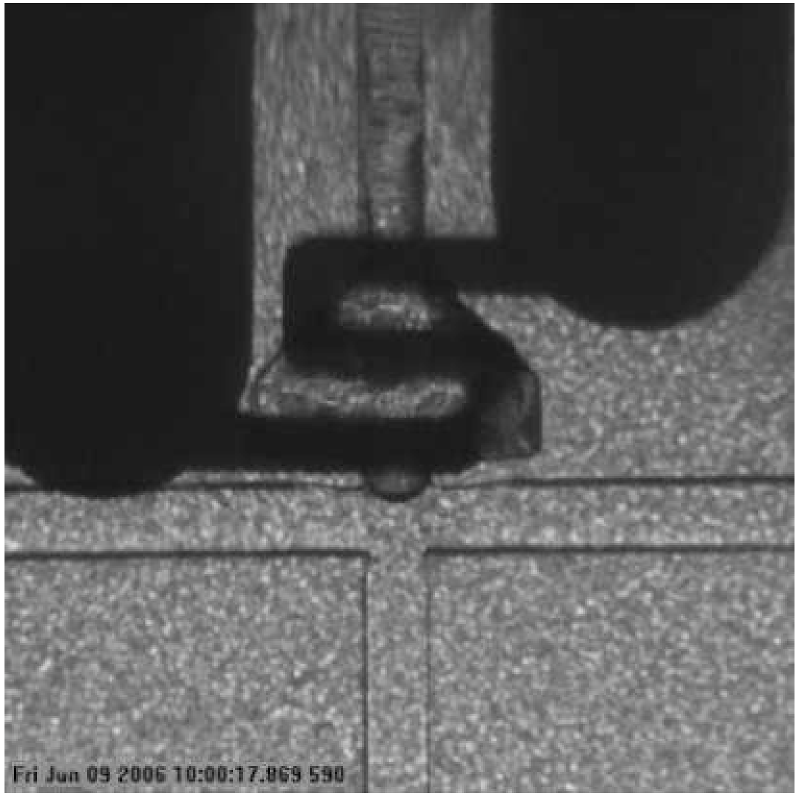

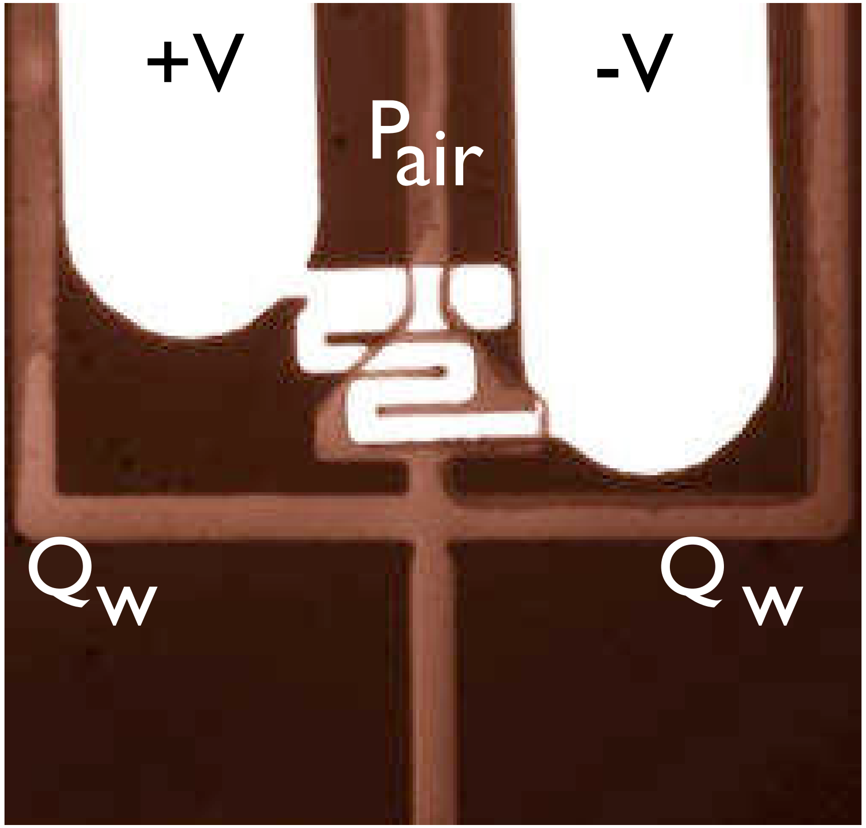

$$\Delta P + \tau = Ca^{-1}k$$
$$Ca = \mu U/\sigma$$

R = 95 Ω, 20V 100ms pulse

Microfluidic Toggle Flip-Flop

- One bit memory
- If T input is “high”, the flip-flop “toggles” state. If T is “low”, the flip-flop holds its state

$$Q_{next} = T \oplus Q$$
$$Q_{next} = T\bar{Q} + \bar{T}Q$$

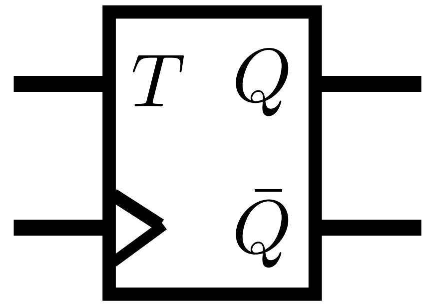

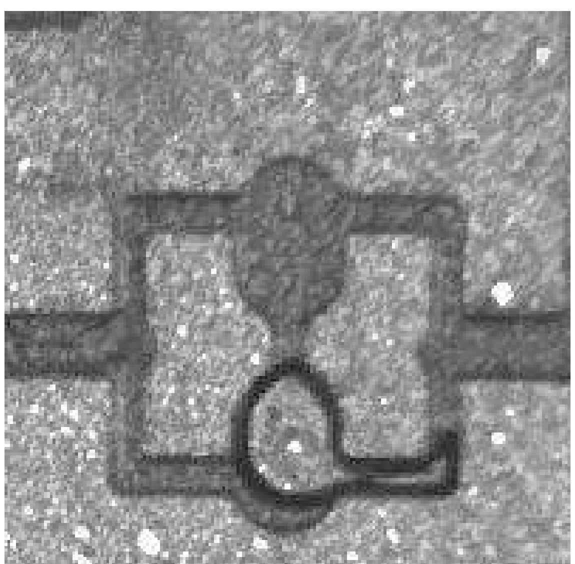

Microfluidic Toggle Flip-Flop

- One bit memory
- If T input is "high", the flip-flop "toggles" state. If T is "low", the flip-flop holds its state

$$Q_{next} = T \oplus Q$$
$$Q_{next} = T\bar{Q} + \bar{T}Q$$

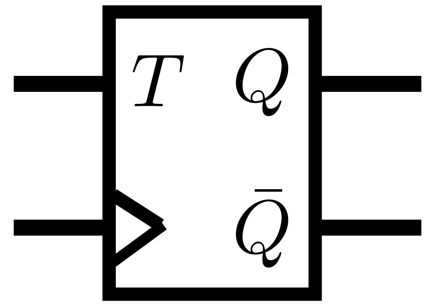

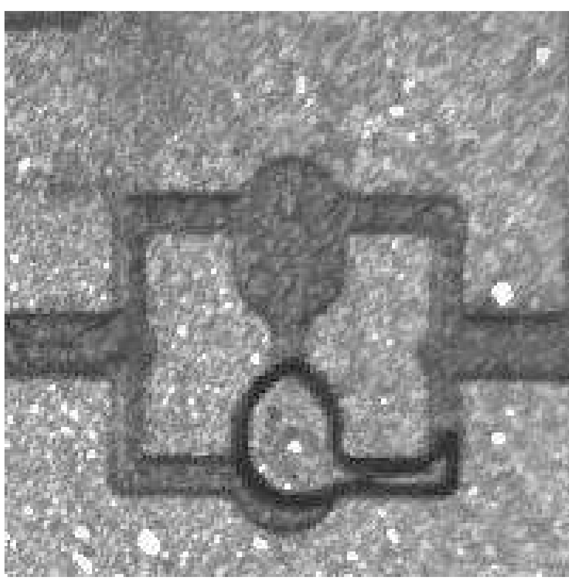

Microfluidic Toggle Flip-Flop

- One bit memory
- If T input is "high", the flip-flop "toggles" state. If T is "low", the flip-flop holds its state

$$Q_{next} = T \oplus Q$$
$$Q_{next} = T\bar{Q} + \bar{T}Q$$

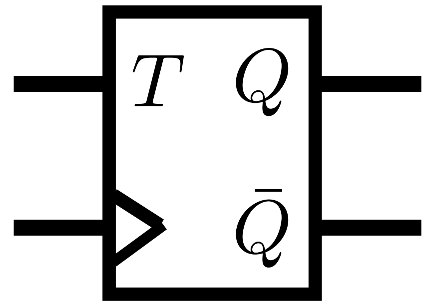

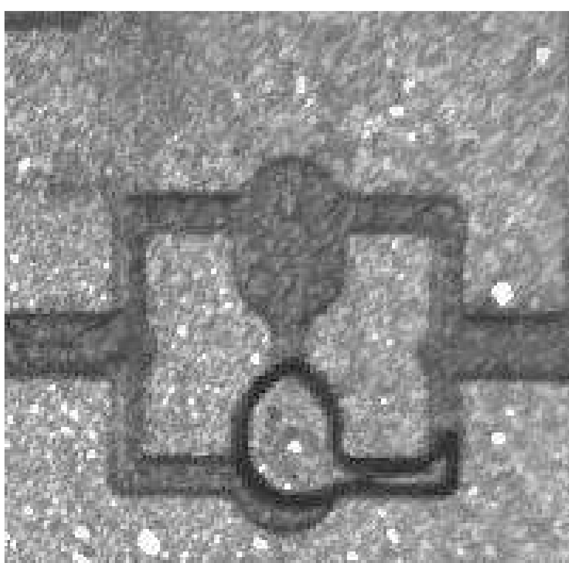

300 fps x1/10

Device Physics

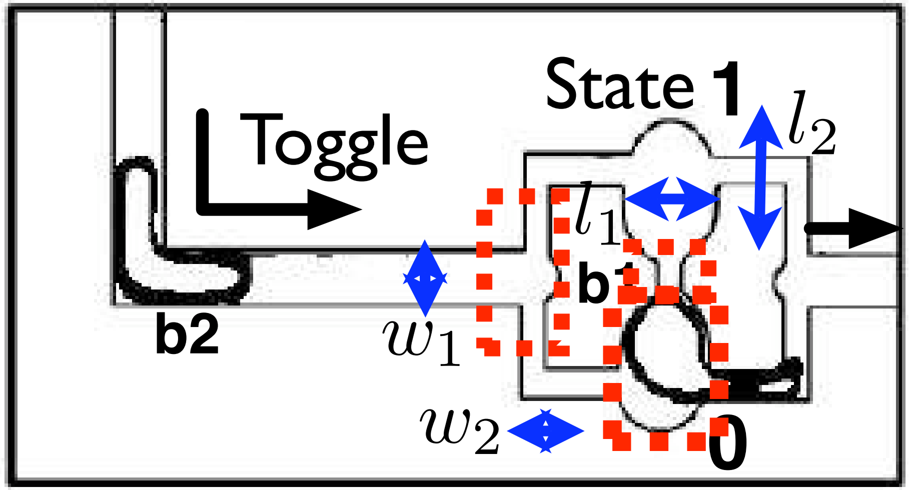

$w_1 = 100\mu m, w_2 = 40\mu m, h = 70\mu m$
$l_1 = 200\mu m, l_2 = 300\mu m$

T junction followed by two elliptical lobes, forming energy minima : Connected via a feedback channel

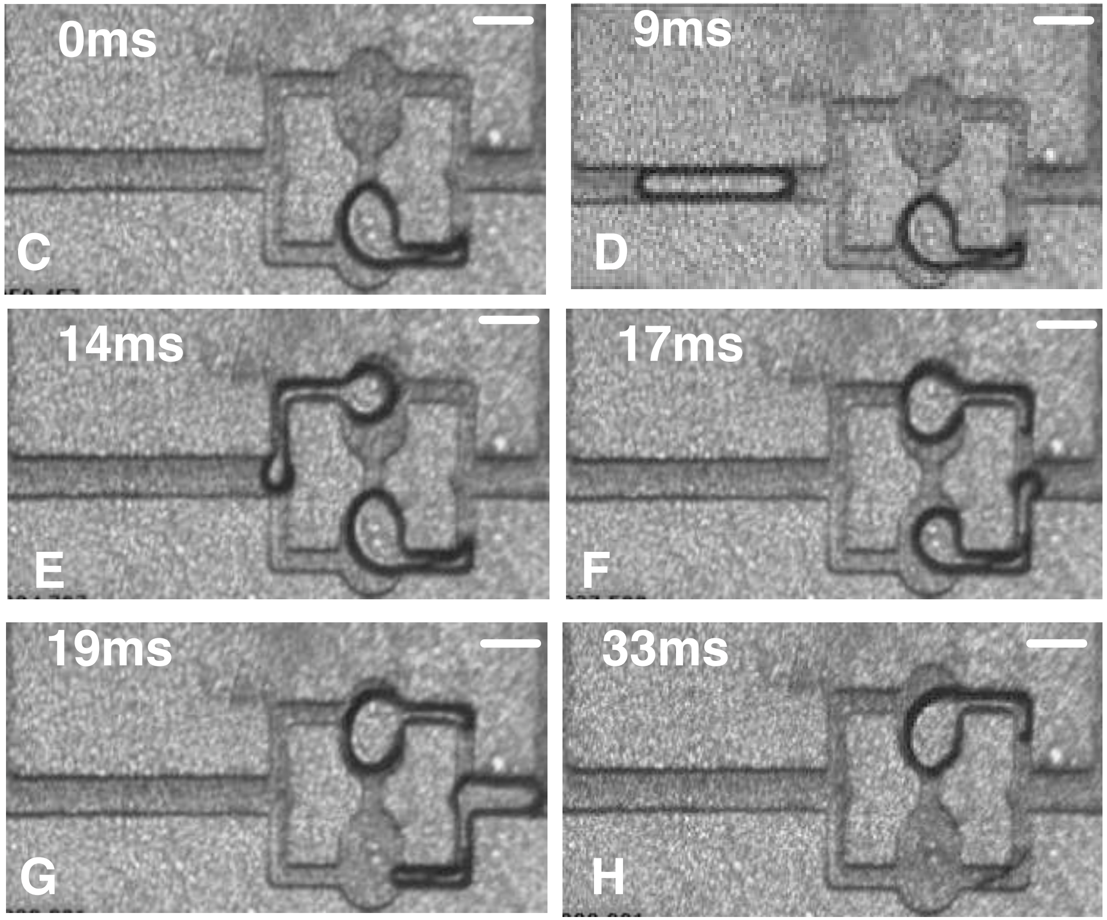

Switching time $\tau = 8ms$

Surface Free Energy

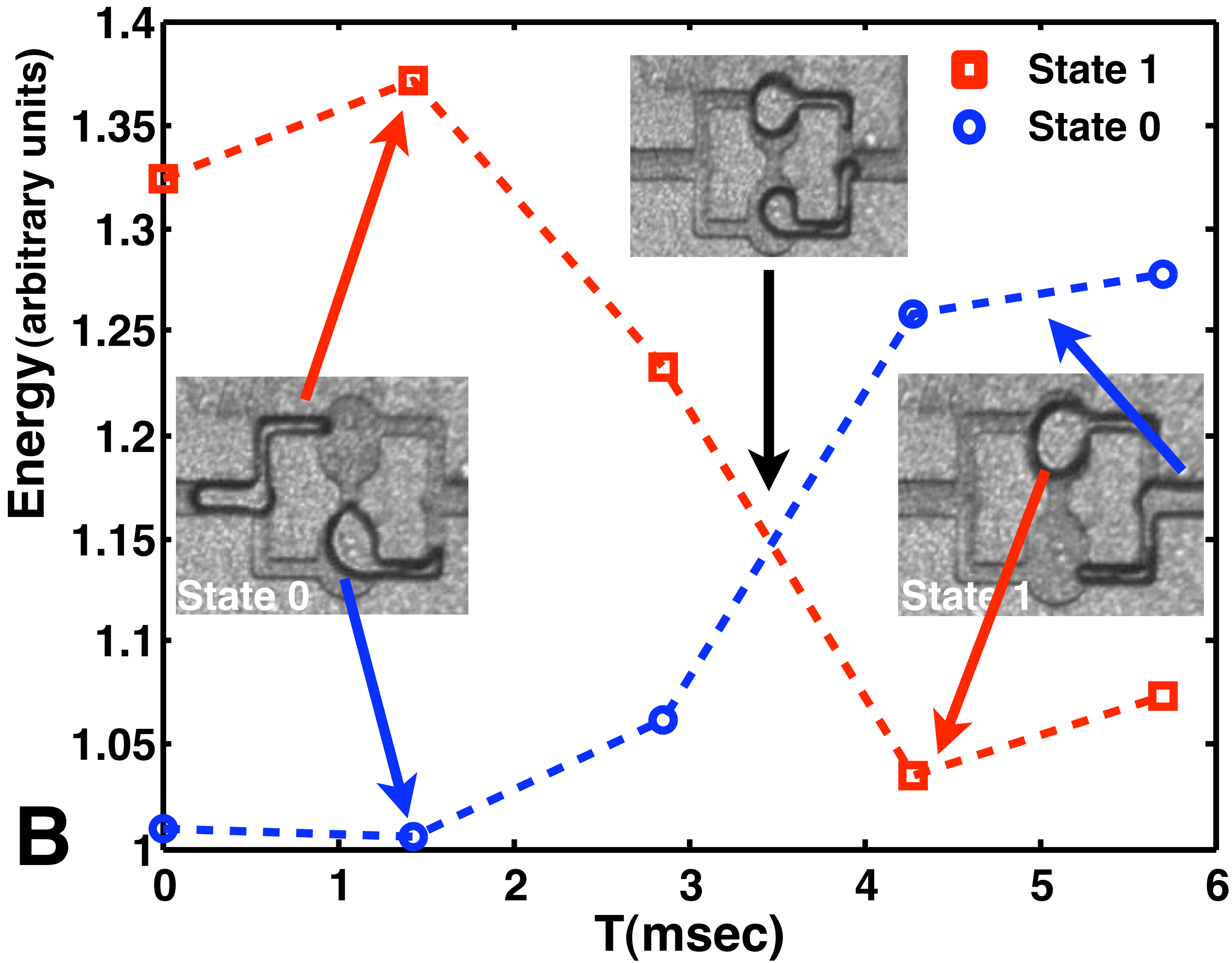

$$S = \sigma_{lg} A$$

$$S \propto P_{perimeter}$$

Bifurcation at T junction

Rayleigh-Plateau breakup at the T junction

$$l/\pi w = 1$$

[H.A. Stone, PRL 2004]

Behavior independent of bubble arrival frequency

[Garstecki, PRE, 2006]

[Ajdari, PRL 2005]

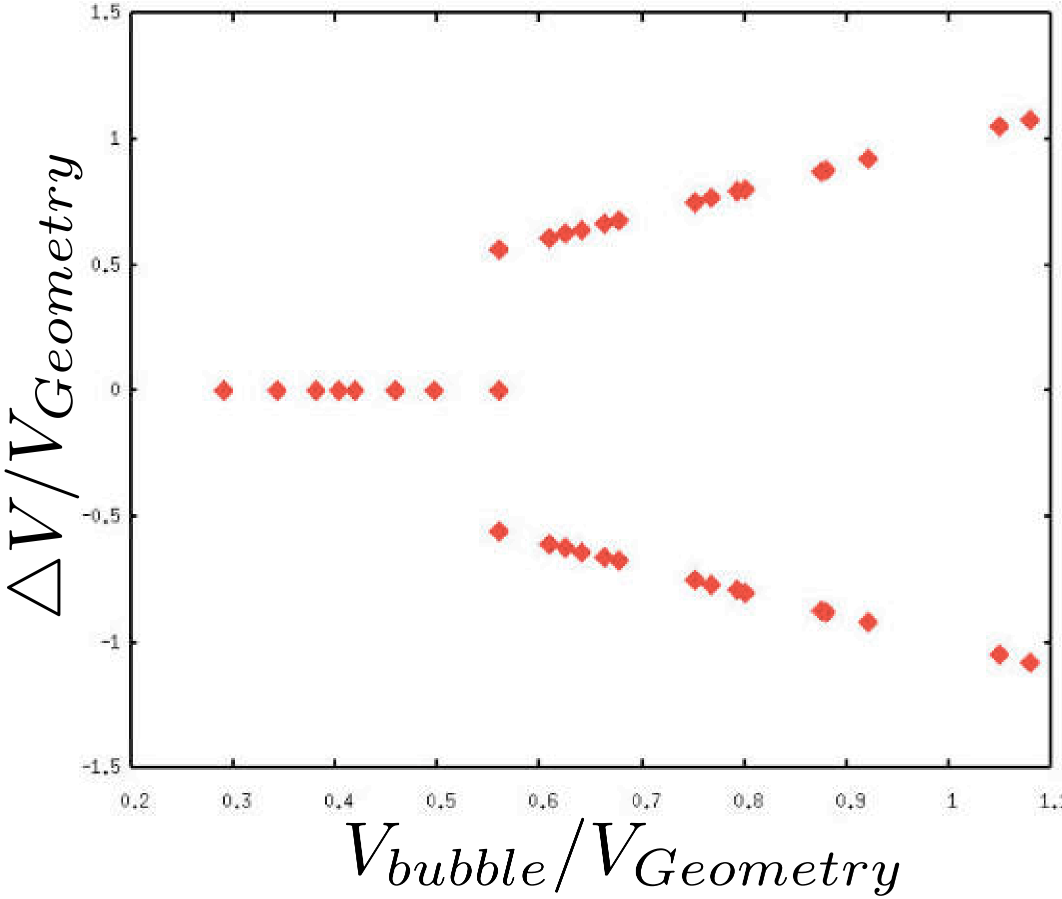

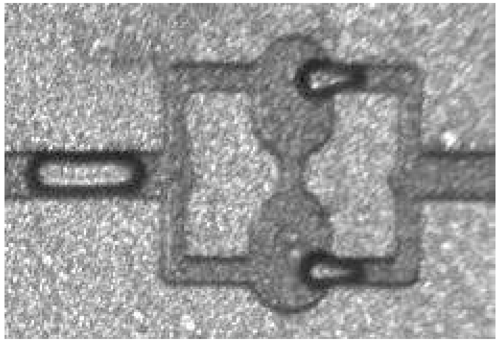

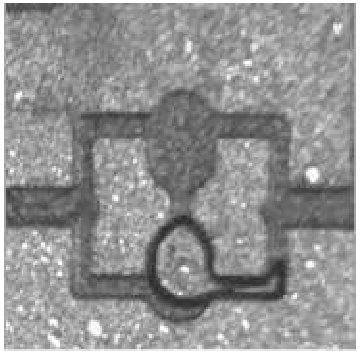

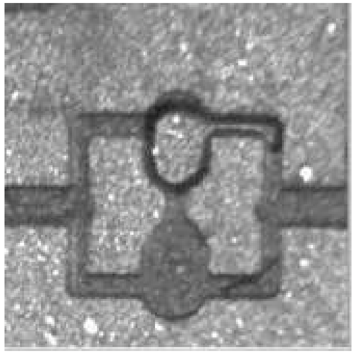

Bifurcation at T junction

Rayleigh-Plateau breakup at the T junction

$$l/\pi w = 1$$

[H.A. Stone, PRL 2004]

Behavior independent of bubble arrival frequency

[Garstecki, PRE, 2006]

[Ajdari, PRL 2005]

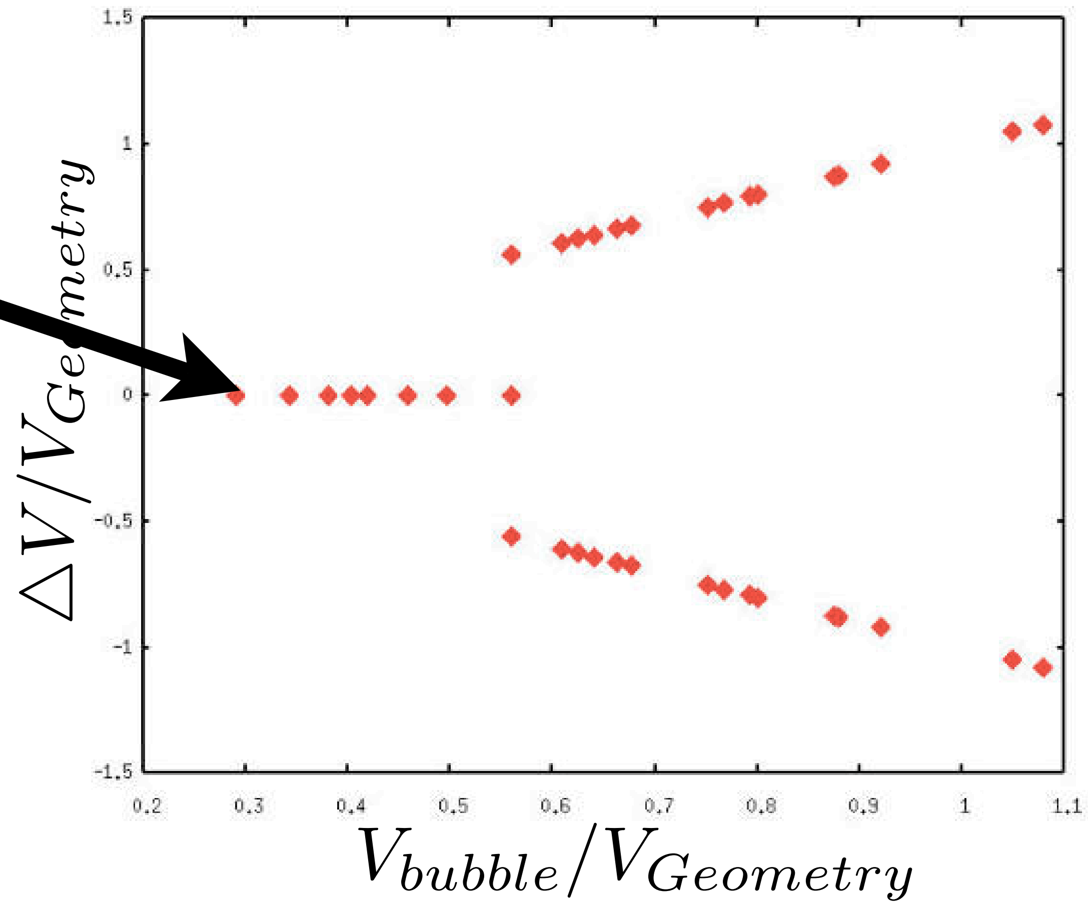

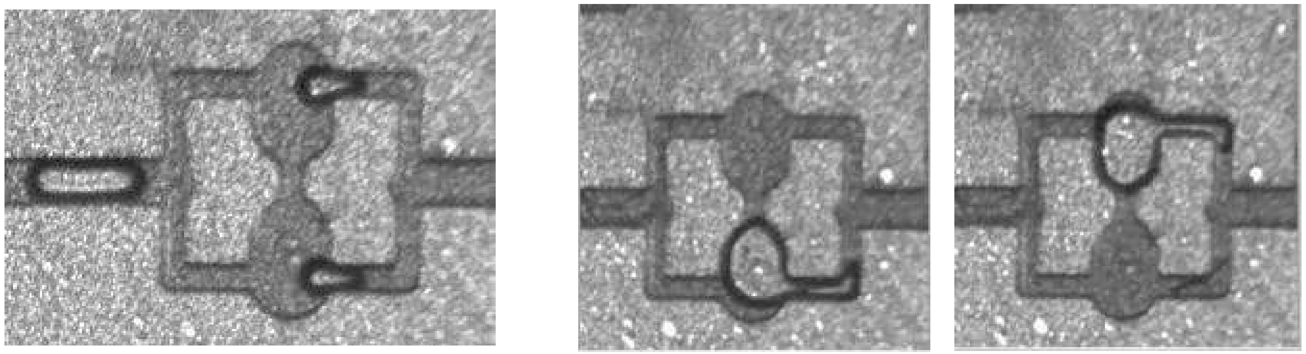

Bifurcation at T junction

Rayleigh-Plateau breakup at the T junction

$$l/\pi w = 1$$

[H.A. Stone, PRL 2004]

Behavior independent of bubble arrival frequency

[Garstecki, PRE, 2006]

[Ajdari, PRL 2005]

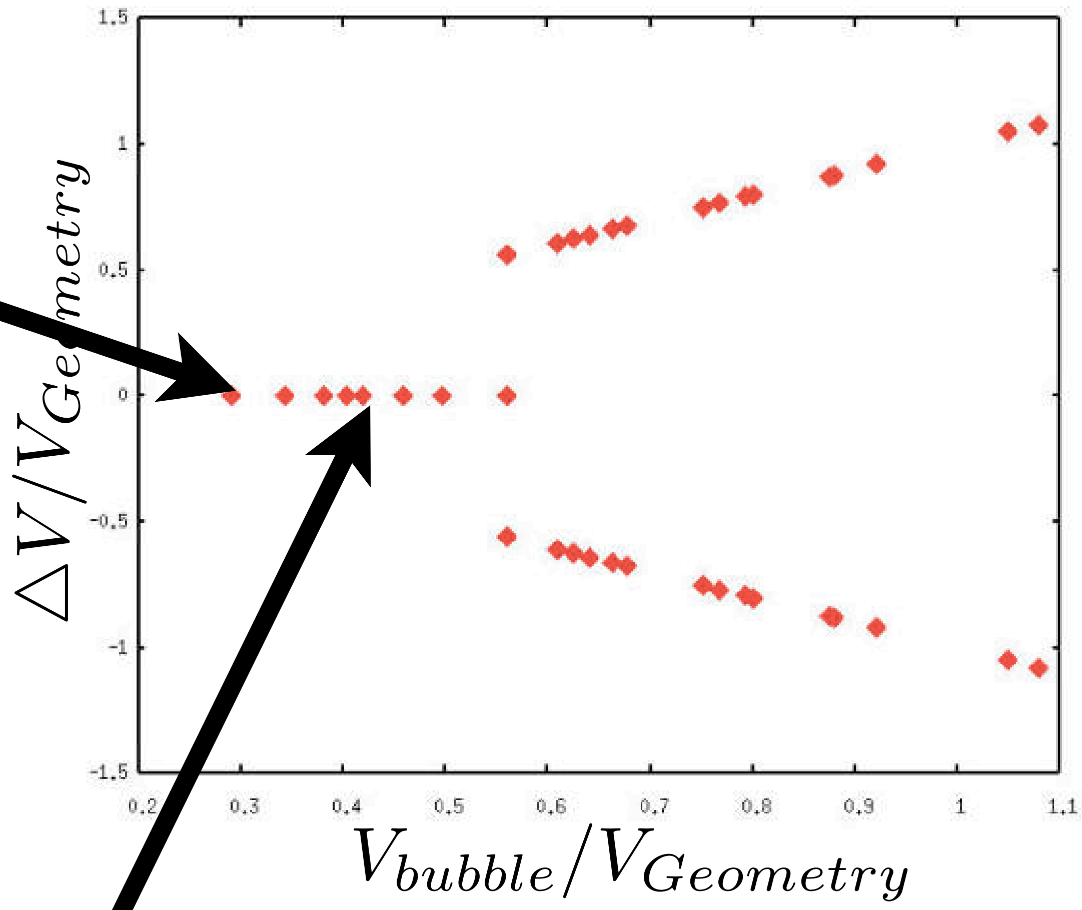

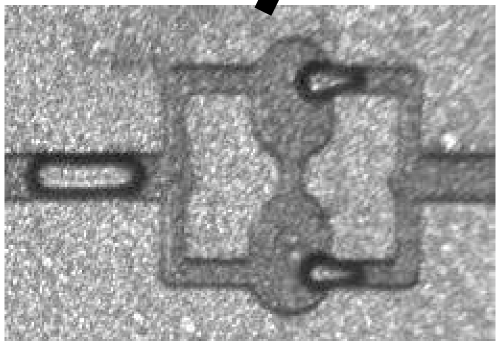

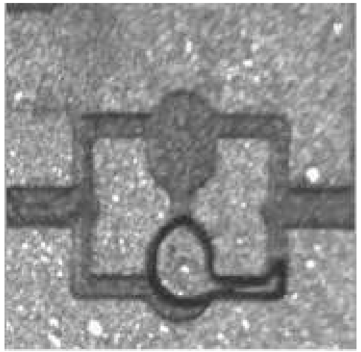

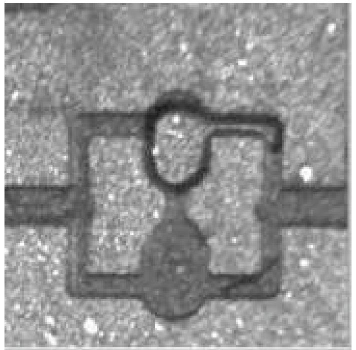

Bifurcation at T junction

Rayleigh-Plateau breakup at the T junction

$$l/\pi w = 1$$

[H.A. Stone, PRL 2004]

Behavior independent of bubble arrival frequency

[Garstecki, PRE, 2006]
[Ajdari, PRL 2005]

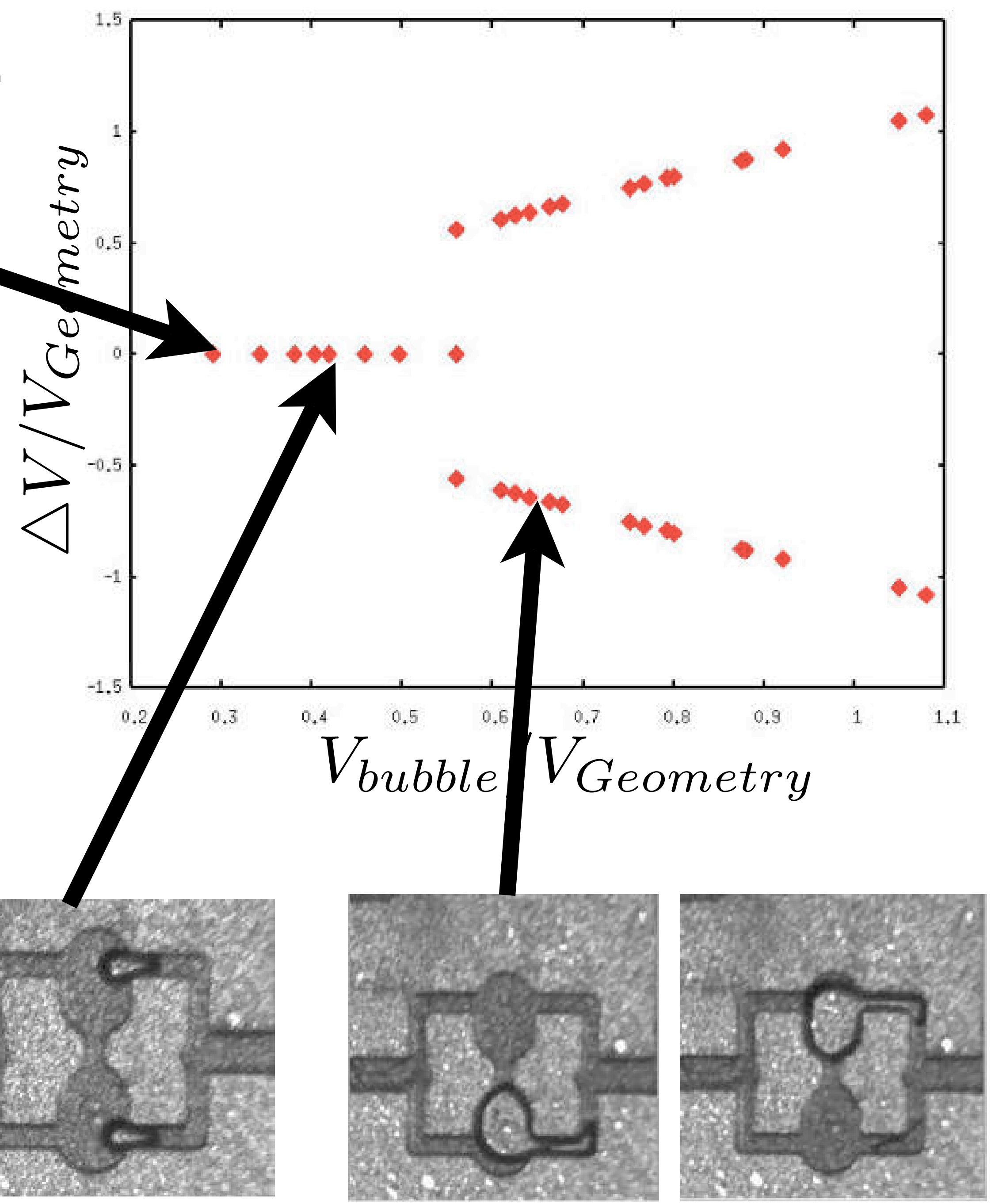

Bifurcation at T junction

Rayleigh-Plateau breakup at the T junction

$$l/\pi w = 1$$

[H.A. Stone, PRL 2004]

Behavior independent of bubble arrival frequency

[Garstecki, PRE, 2006]

[Ajdari, PRL 2005]

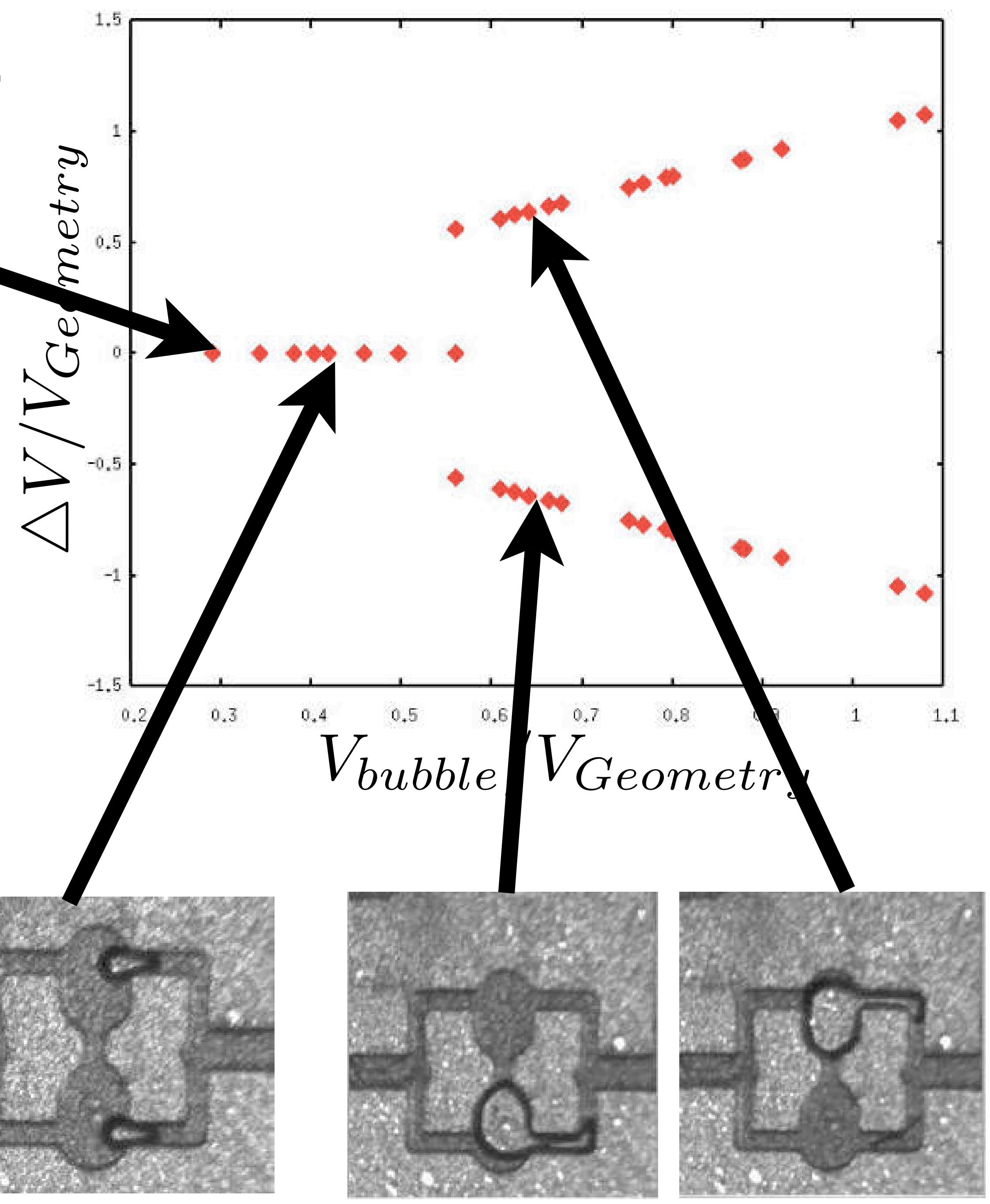

Trap repeatability

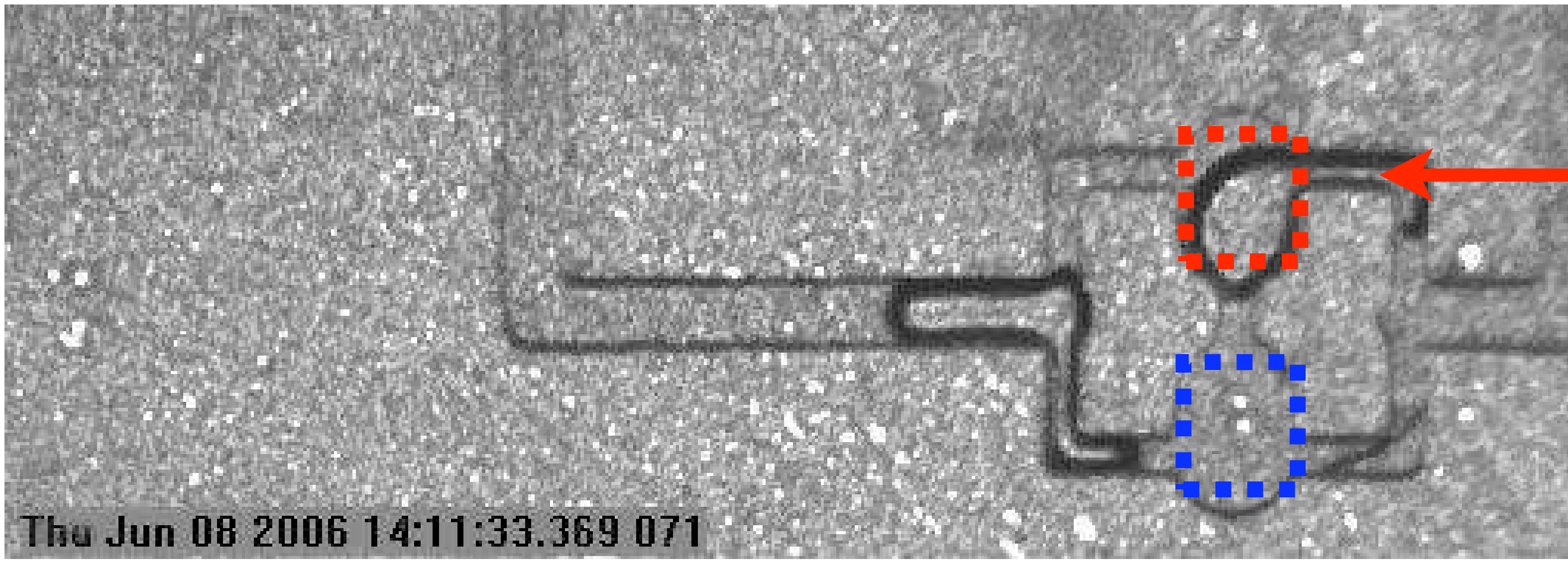

10Hz bistable one-bit memory

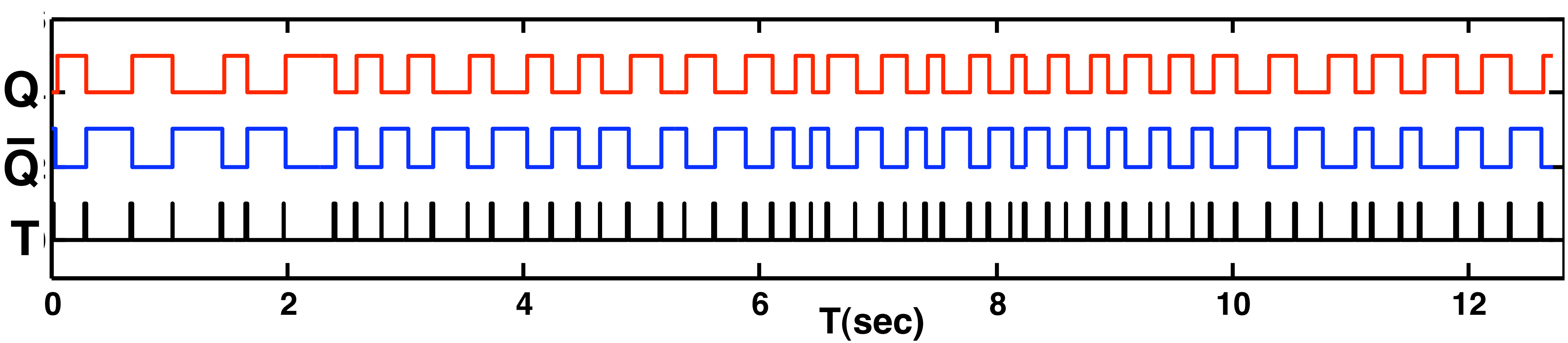

Applications

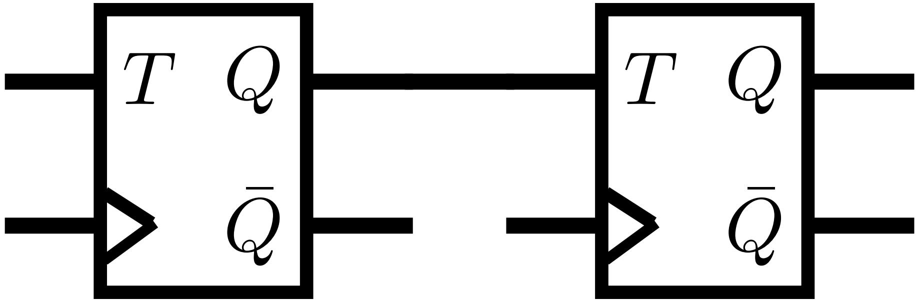

Counting drops

RIPPLE COUNTER

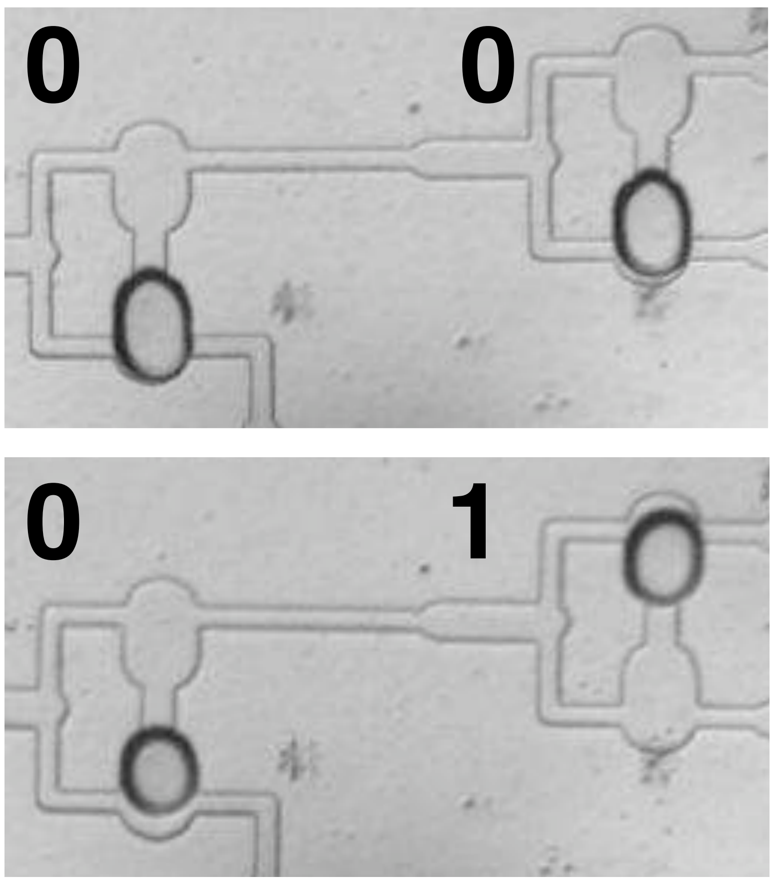

High speed switching valves

BISTABLE VALVES

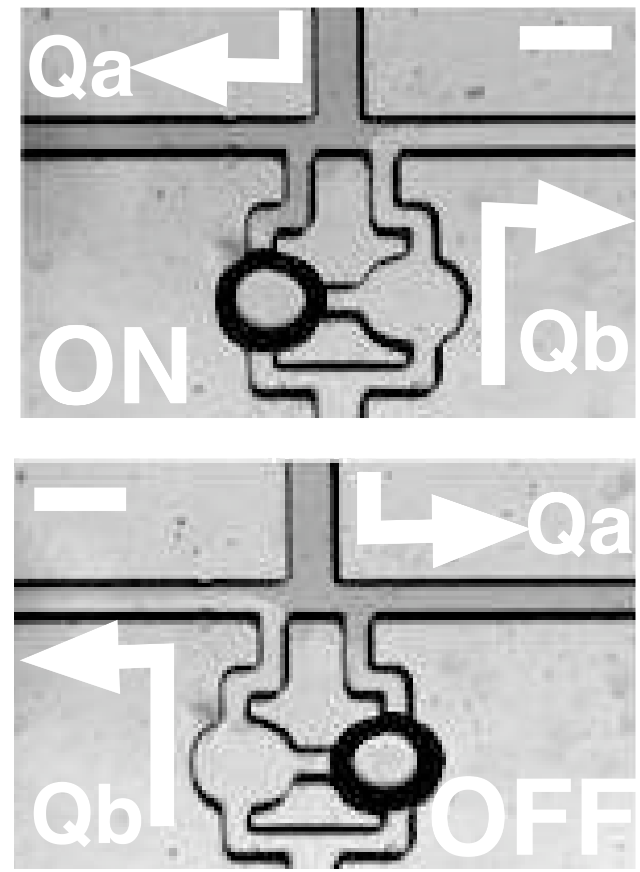

Inverter

Designed as
NOT(A).B gate for B=1

INVERTER WITH GAIN

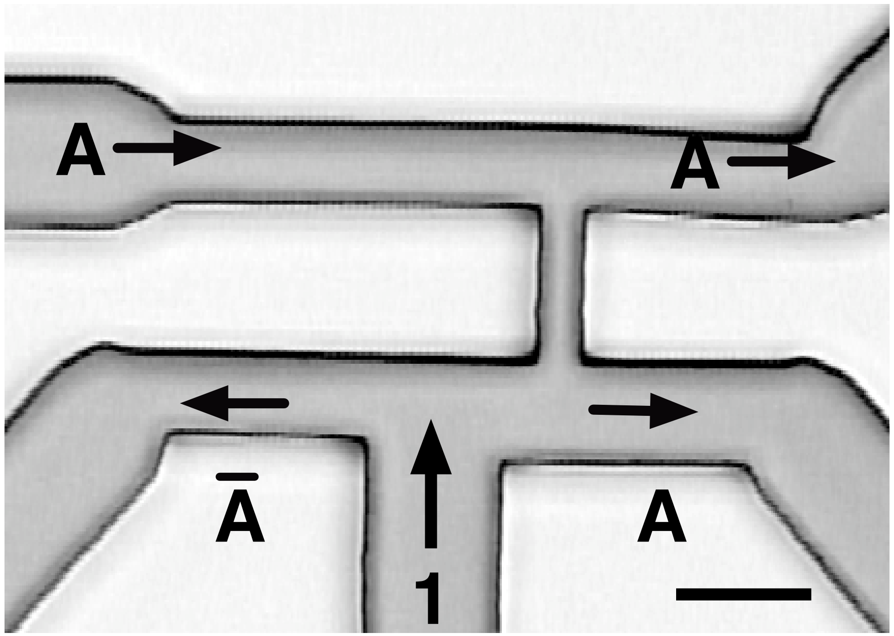

Scale bar $100\mu m$

Fredkin gate (reversible logic)

Inverter

Designed as NOT(A).B gate for B=1

INVERTER WITH GAIN

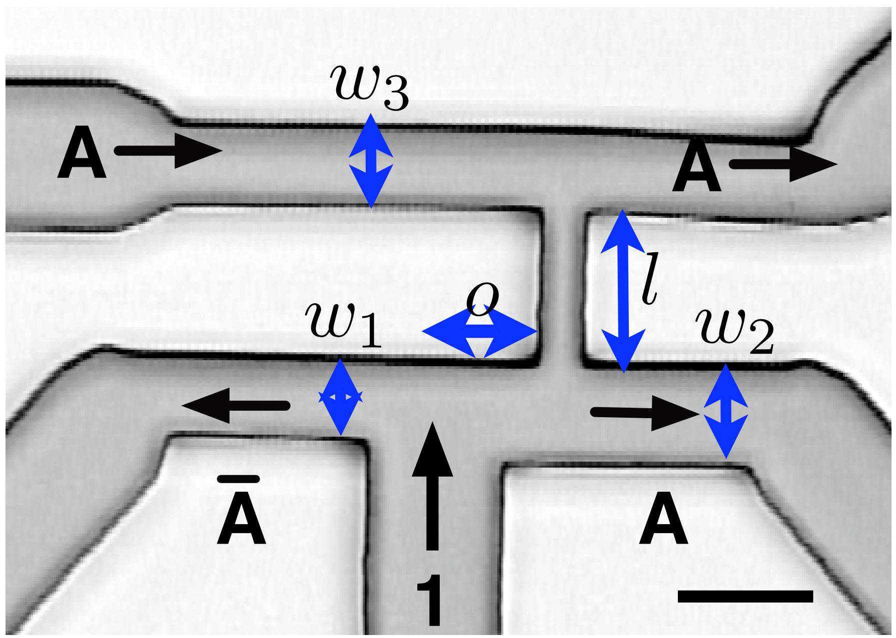

$w_2 > w_1$

Scale bar $100\mu m$

Fredkin gate (reversible logic)

Inverter

Designed as NOT(A).B gate for B=1

INVERTER WITH GAIN

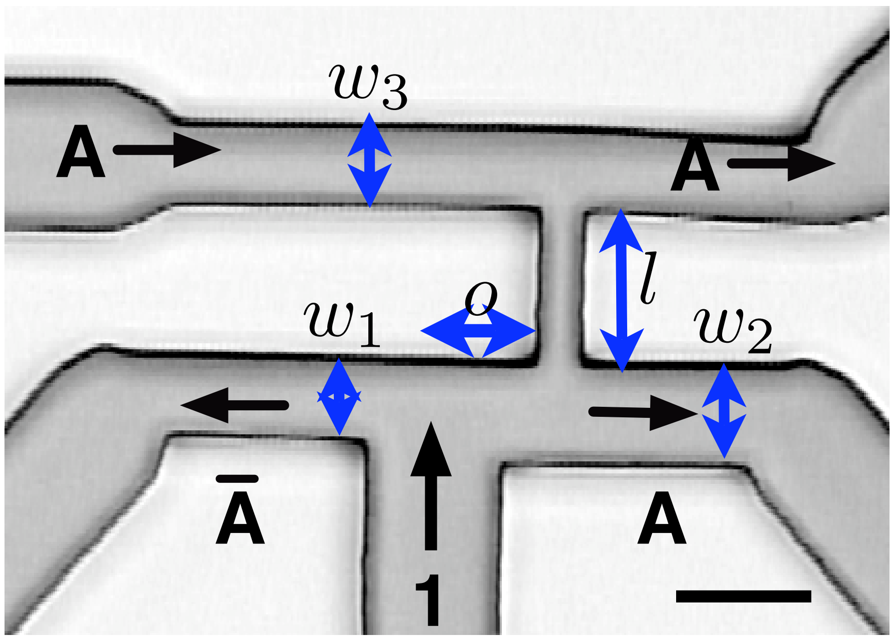

$w_2 > w_1$ Scale bar $100\mu m$

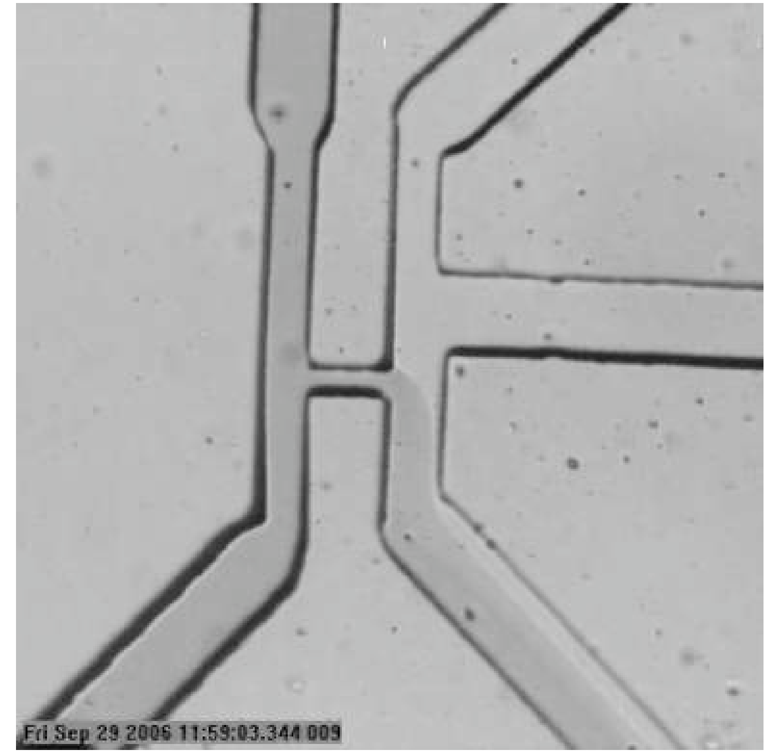

Fredkin gate (reversible logic)

Inverter

Designed as NOT(A).B gate for B=1

A=0
B=1
NOT(A)=1

INVERTER WITH GAIN

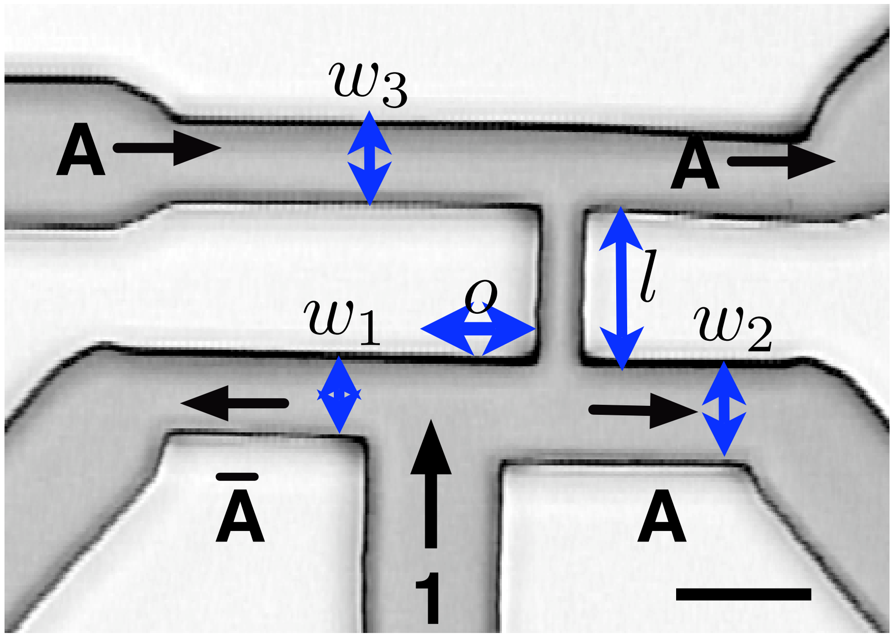

$w_2 > w_1$ Scale bar $100\mu m$

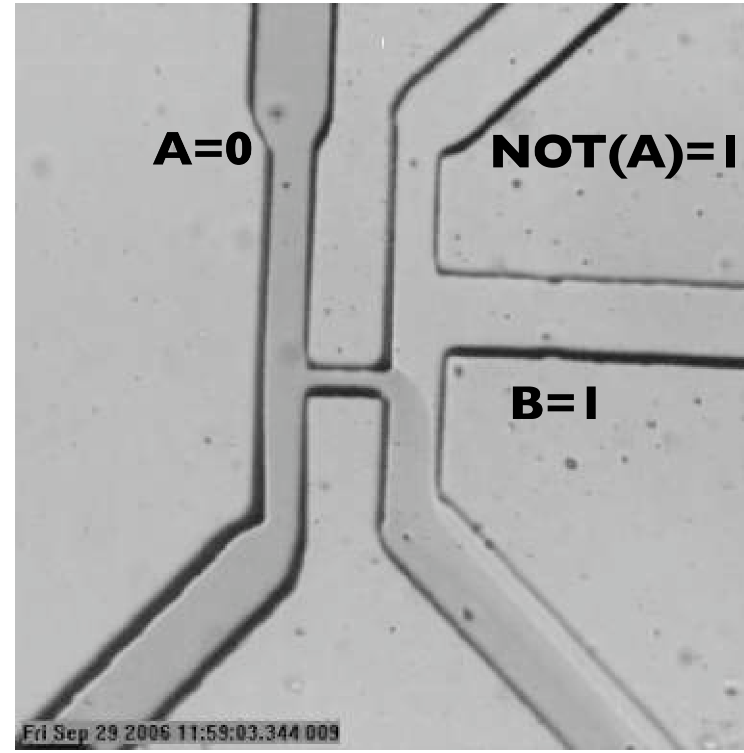

Fredkin gate (reversible logic)

Inverter

Designed as NOT(A).B gate for B=1

INVERTER WITH GAIN

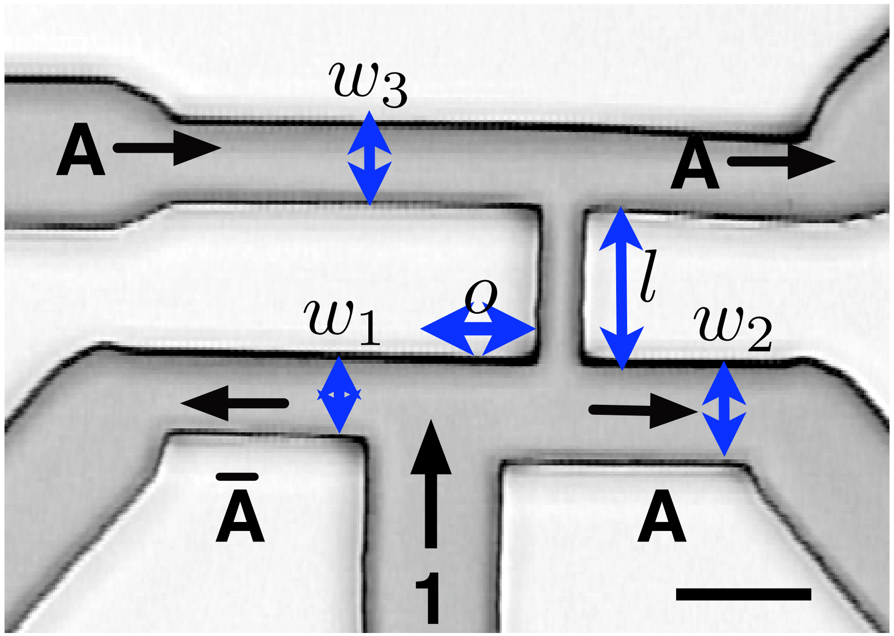

$w_2 > w_1$

Scale bar $100\mu m$

A=0
B=1
NOT(A)=1

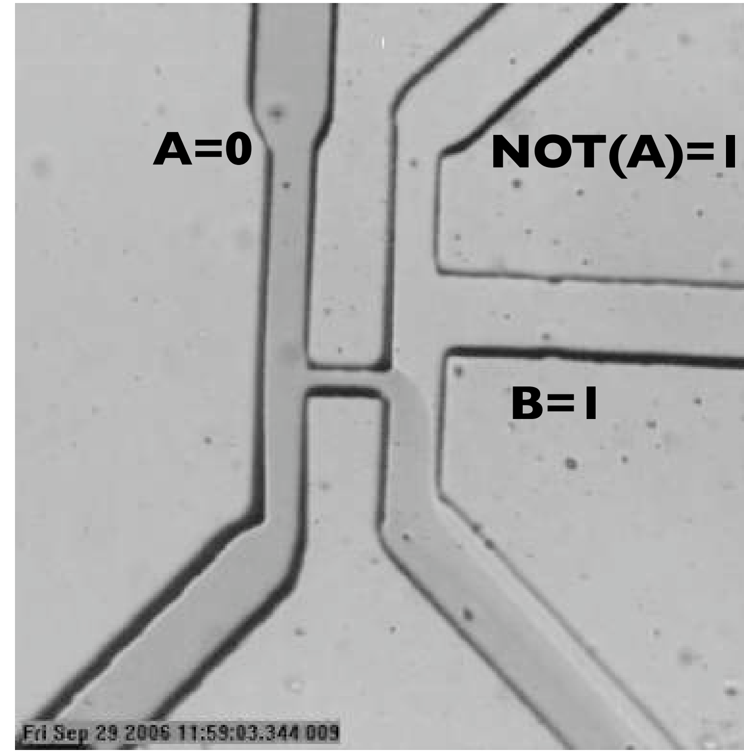

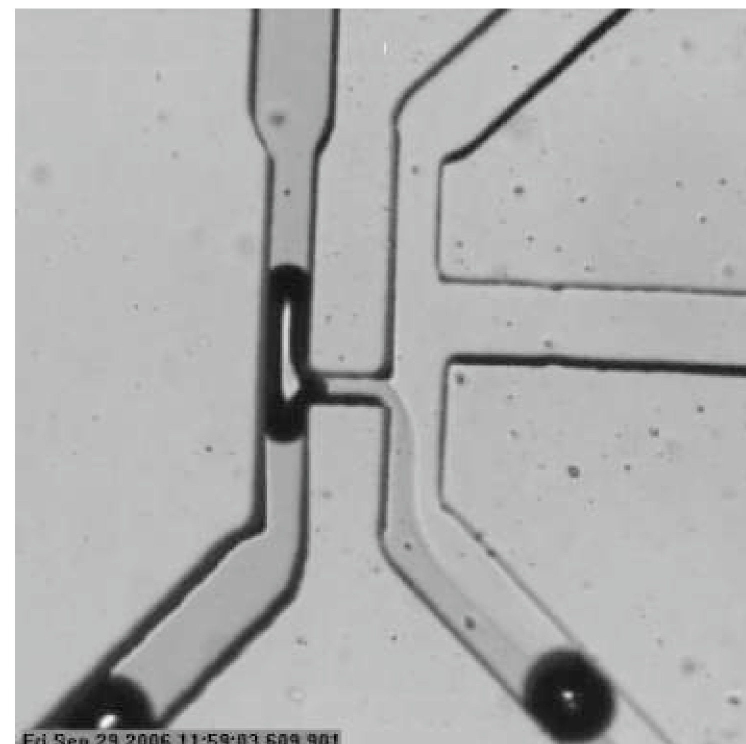

Fredkin gate (reversible logic)

Inverter

Designed as
NOT(A).B gate for B=1

INVERTER WITH GAIN

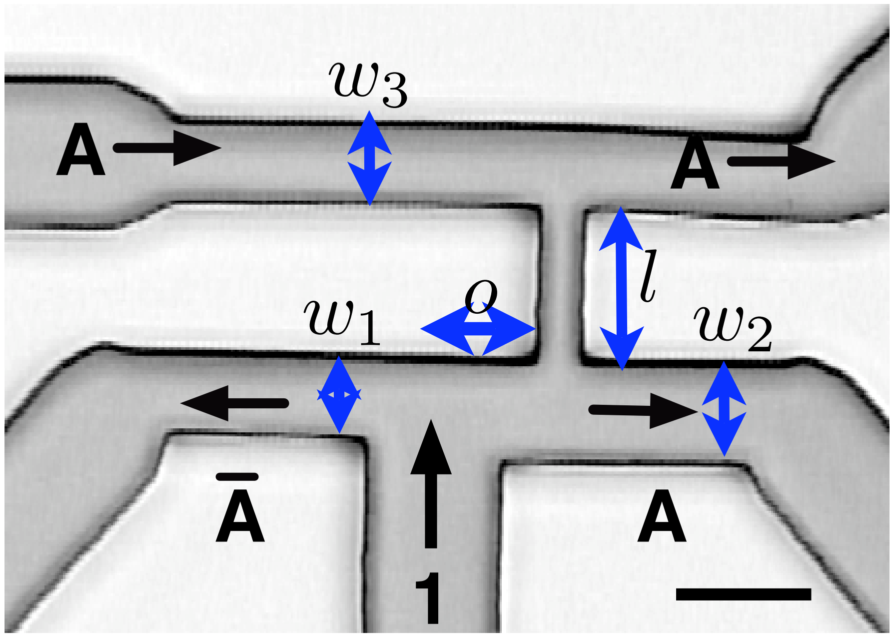

$w_2 > w_1$ Scale bar $100\mu m$

A=0
B=1
NOT(A)=1

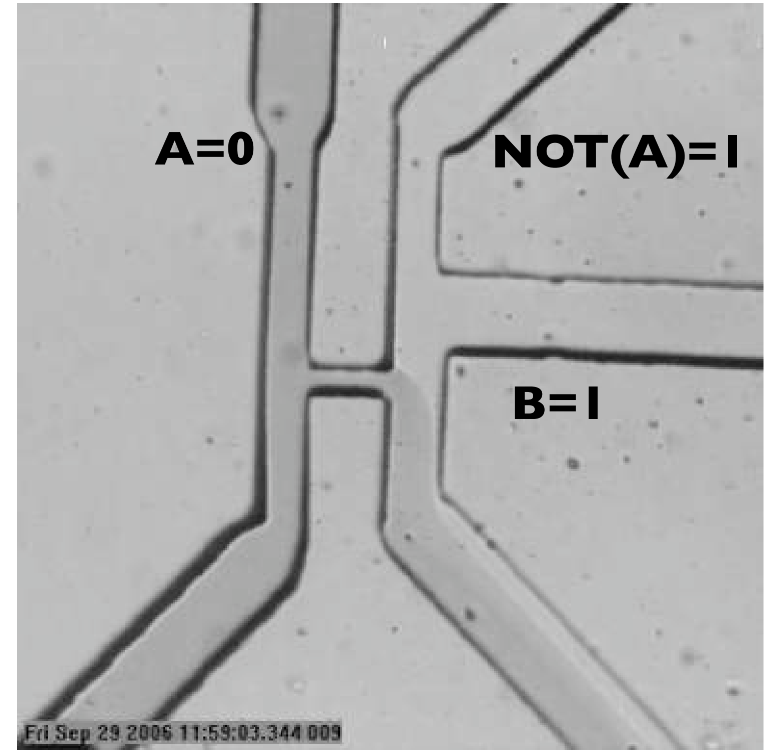

A=1
B=1
NOT(A)=0

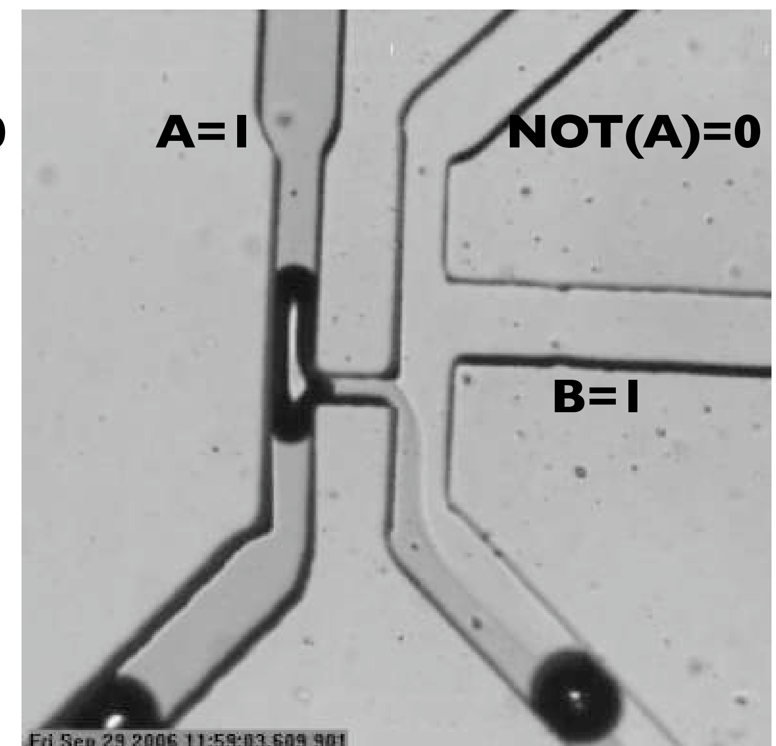

Fredkin gate
(reversible
logic)

Inverter : amplification/gain

Dependence on bubble length
- Viscous dissipation in thin continuos fluid film
- Viscous dissipation in dispersed phase

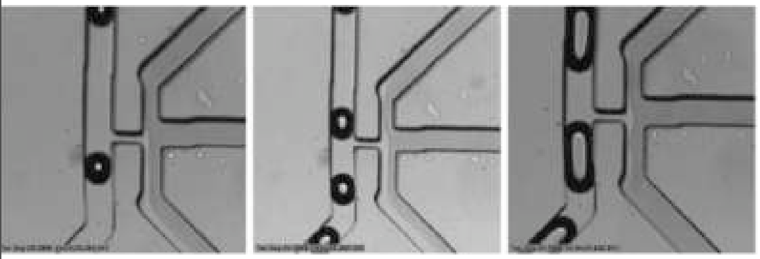

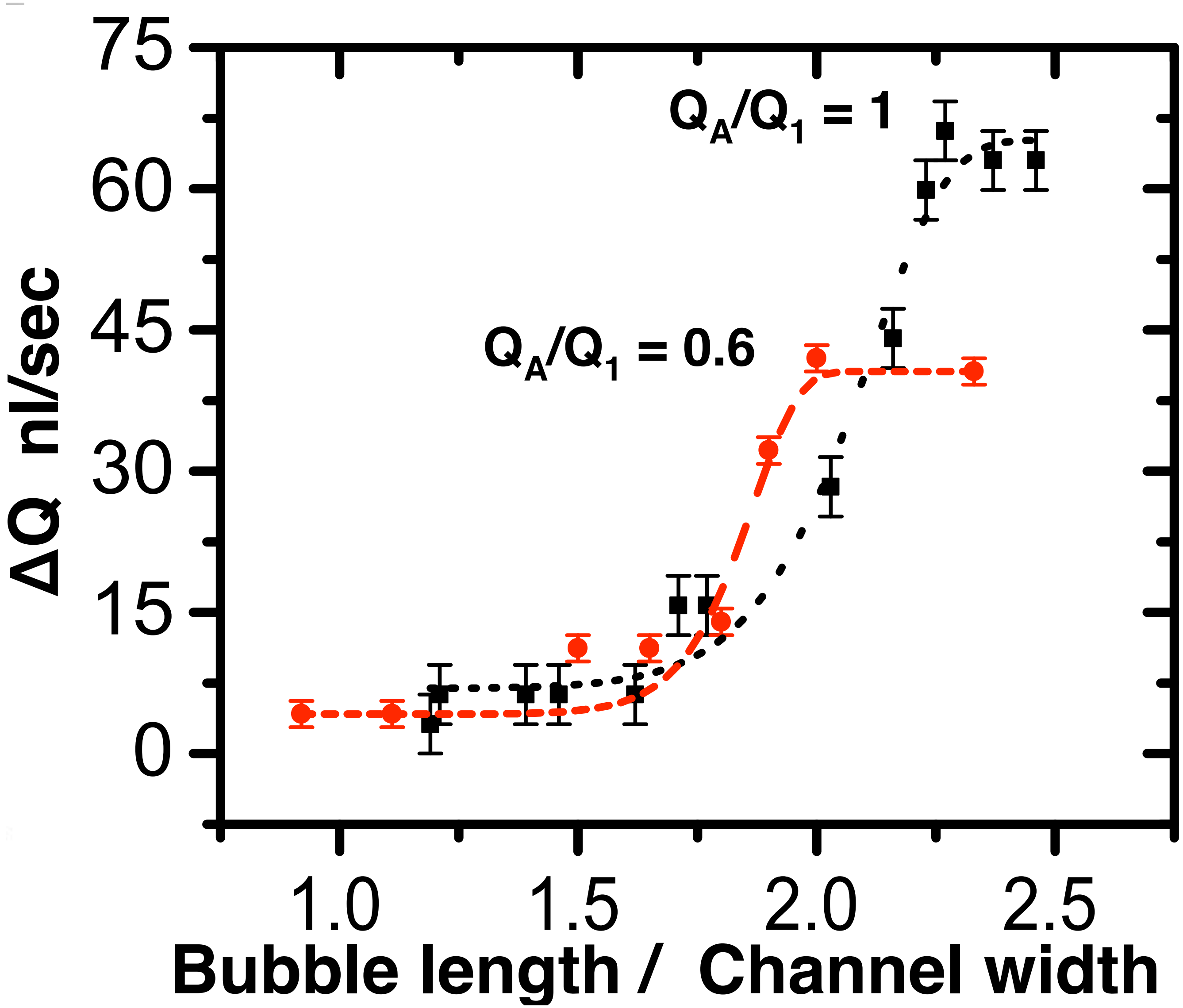

Bubble/Bit synchronizer

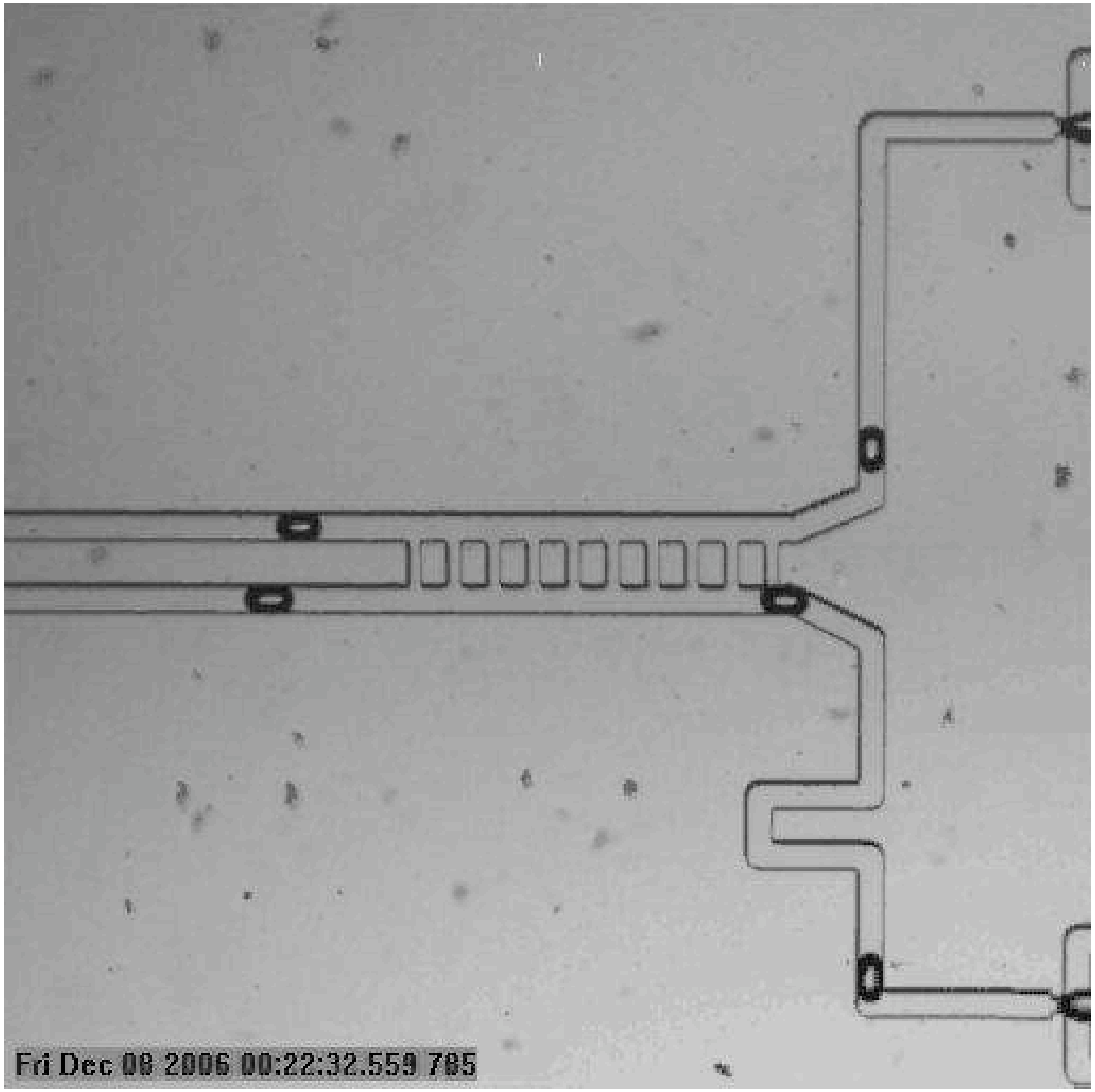

1000 fps
high speed
video

Non-linear ladder network

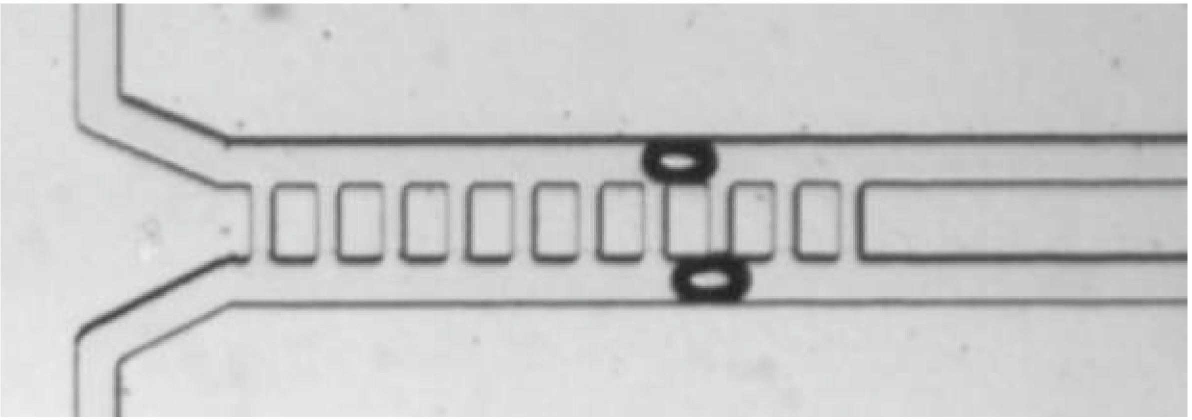

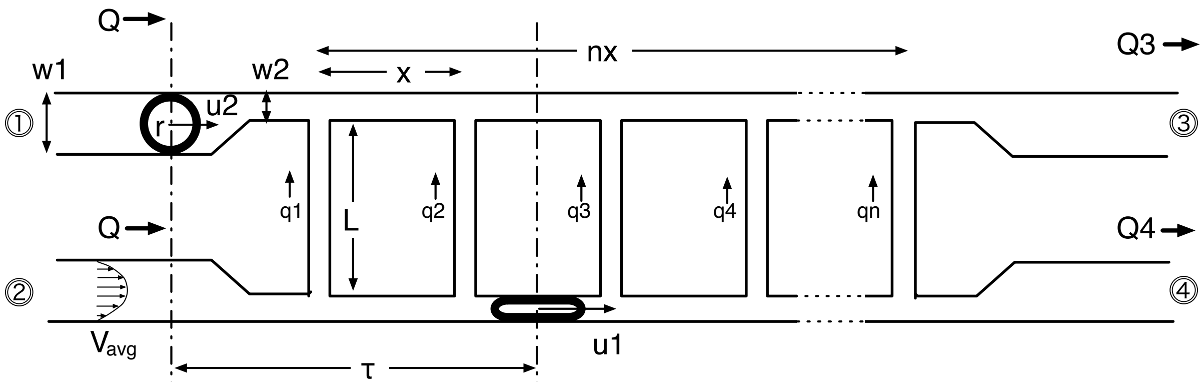

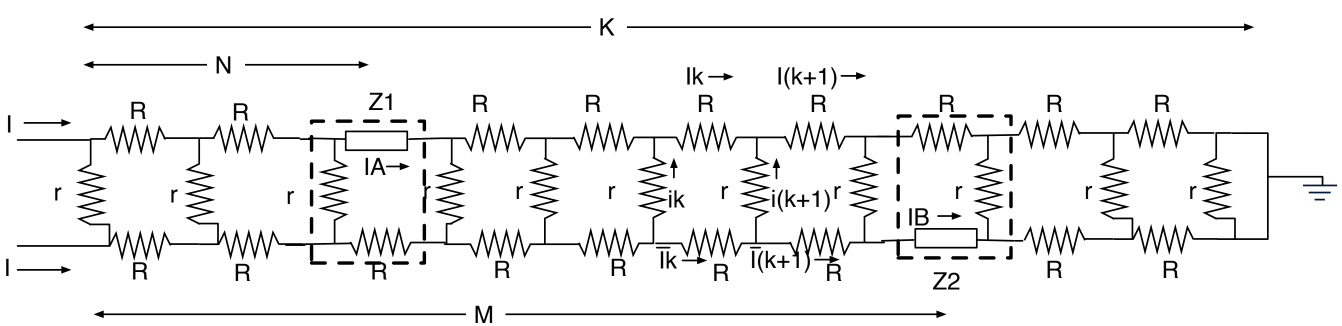

Parameters

- r/R relative flow resistance
- m,n state of the device
- k number of channels
- I constant injected flow

$$U_A - U_B = f(r/R, m, n, k, I)$$

$$I_j - \bar{I}_j = \frac{r}{R}(i_{j+1} - i_j)$$

$$I_j - I_{j-1} = i_j$$

$$\bar{I}_j - \bar{I}_{j-1} = -i_j$$

$$I_j = I_{j-1} + 2\frac{R}{r}S_{j-1}$$

$$I_j = 2\frac{R+r}{r}I_{j-1} - I_{j-2}$$

where $S_{j-1} = \sum I_{j-1}$

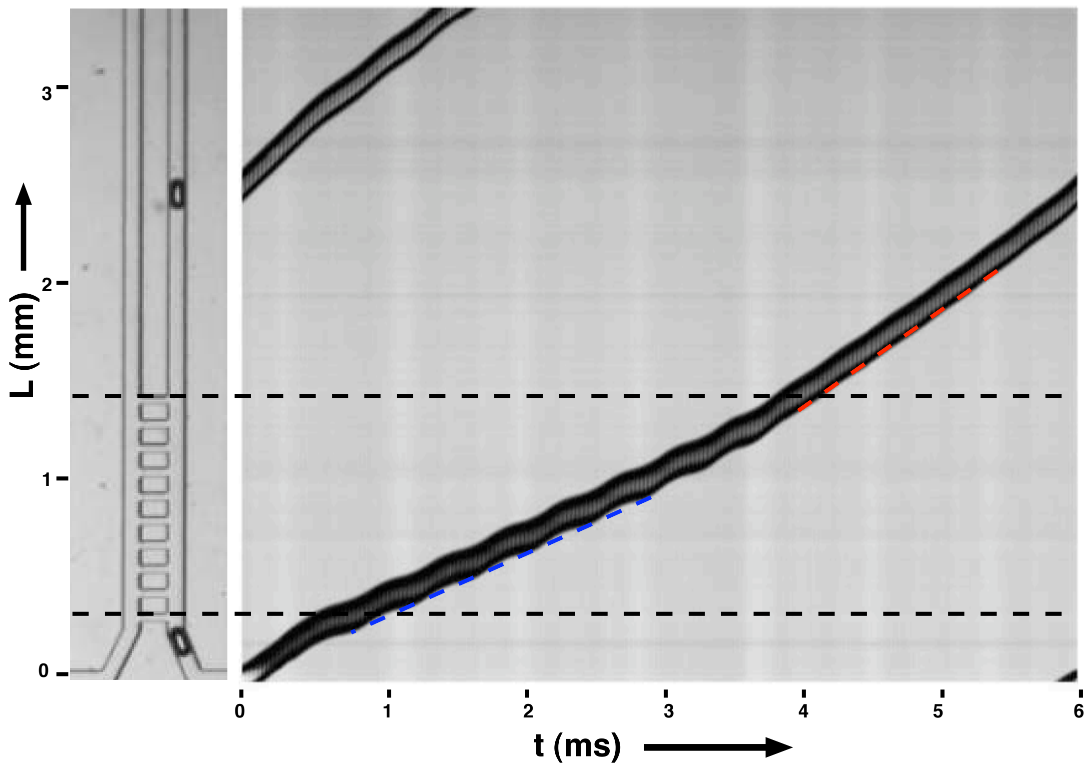

L (mm)
t (ms)
0
1
2
3
4
5
6

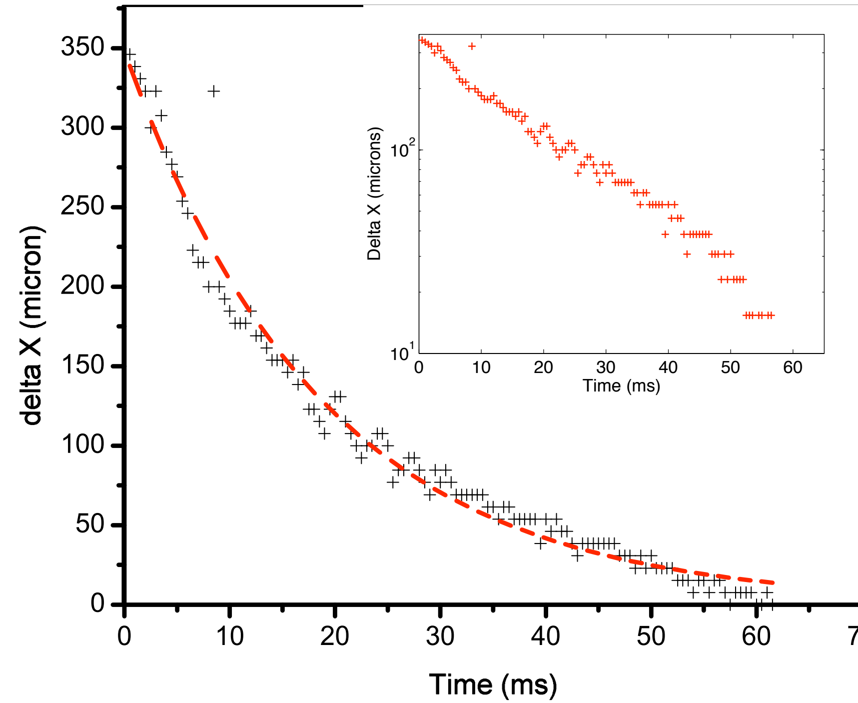

delta X (micron)
Time (ms)
Delta X (microns)
Time (ms)

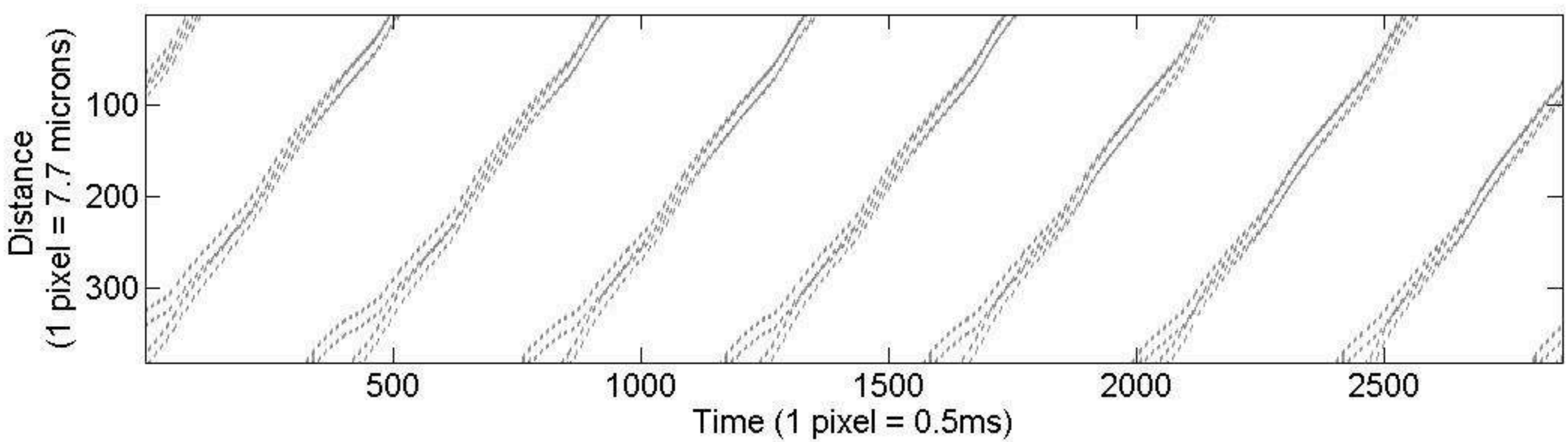

Distance
(1 pixel = 7.7 microns)
Time (1 pixel = 0.5ms)

Designing microfluidic circuits

What if we connect three AND gates and three delay lines .. in a ring?

Designing microfluidic circuits

What if we connect three AND gates and three delay lines .. in a ring?

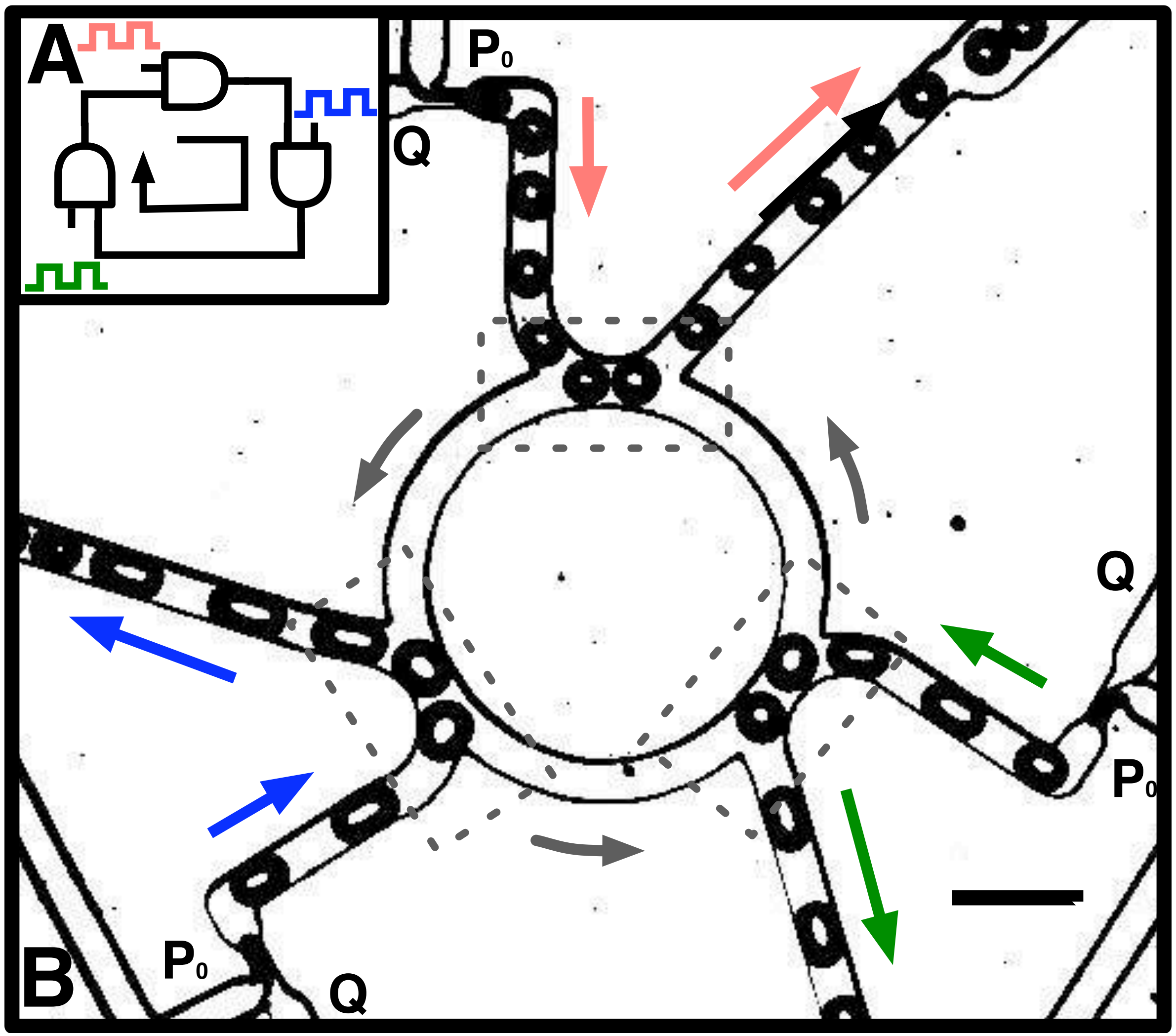

Ring Oscillator

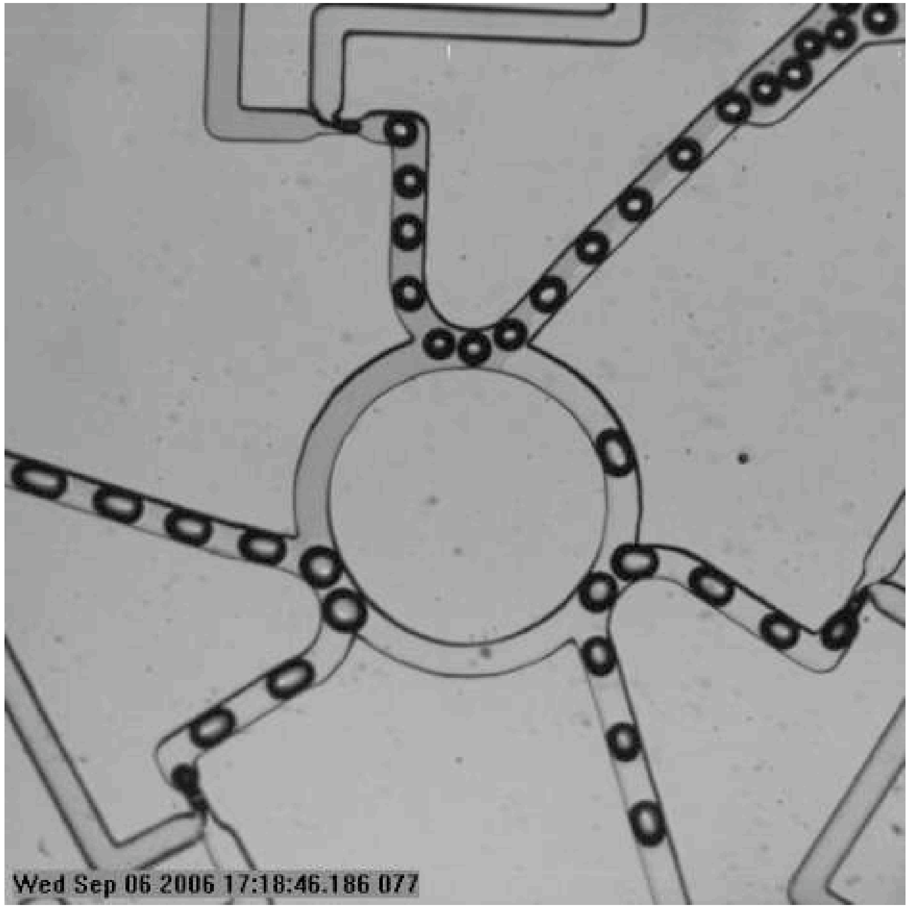

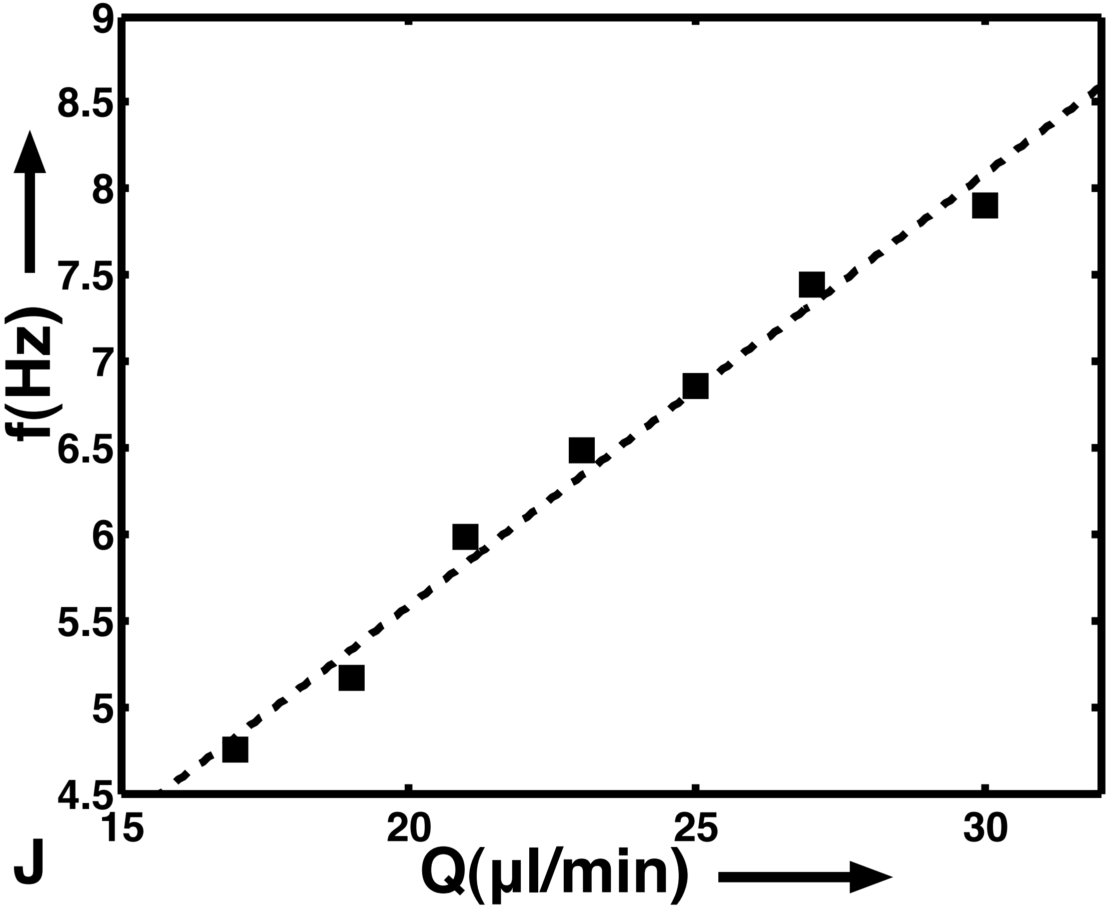

Frequency dependence

$$f \propto 1/[3(l/v + \tau_d)]$$

NONLINEARITY

AND/OR gate

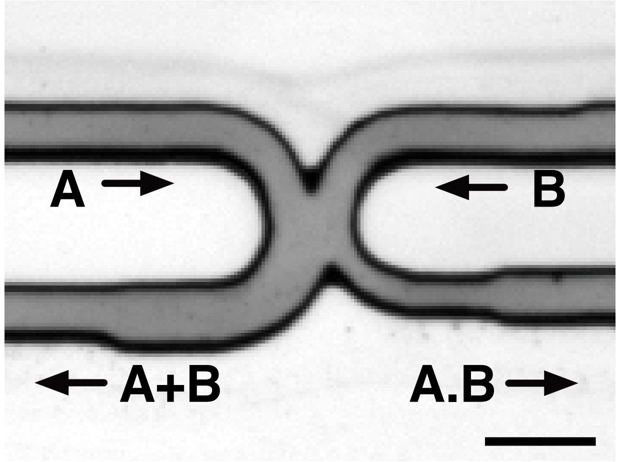

NONLINEARITY

AND/OR gate

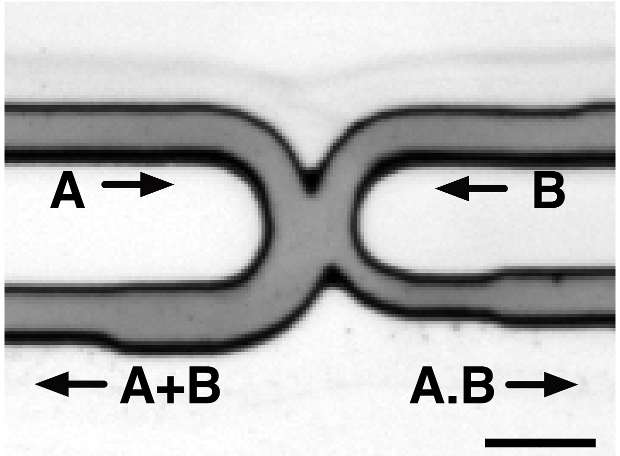

NOT gate

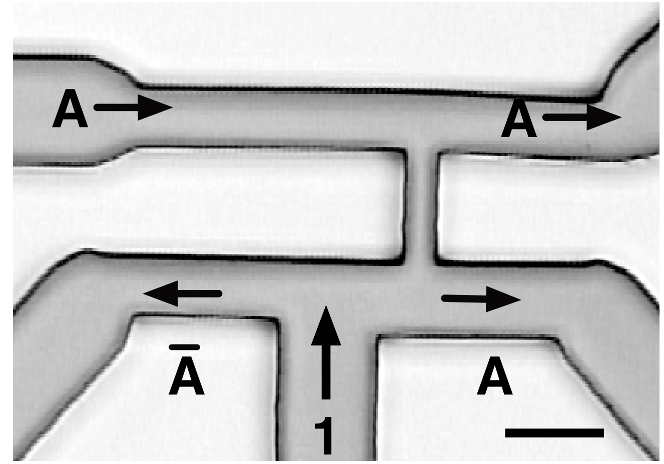

GAIN
INVERSION

NONLINEARITY

AND/OR gate

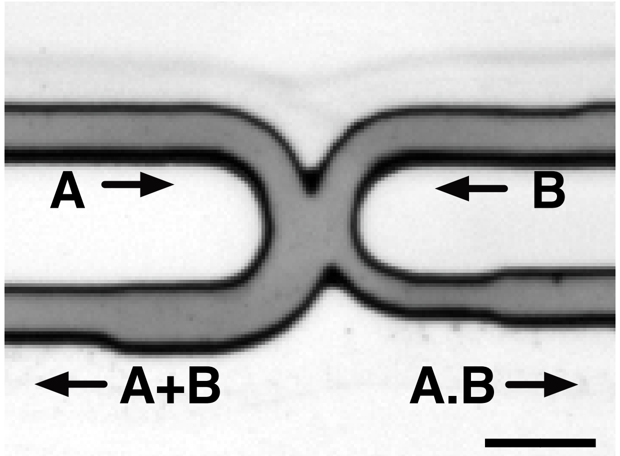

NOT gate

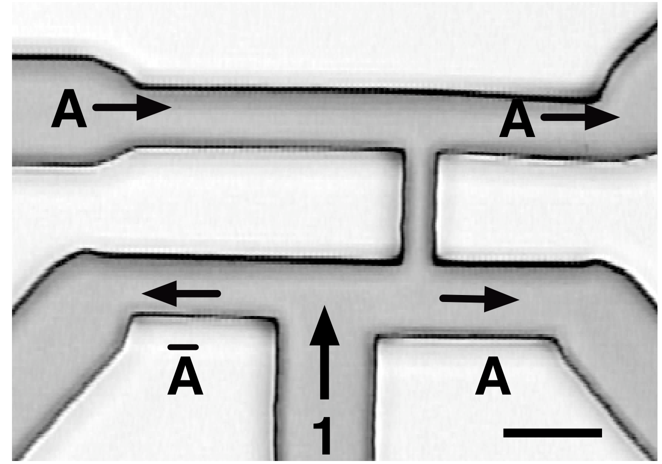

GAIN INVERSION

Toggle Flip-Flop

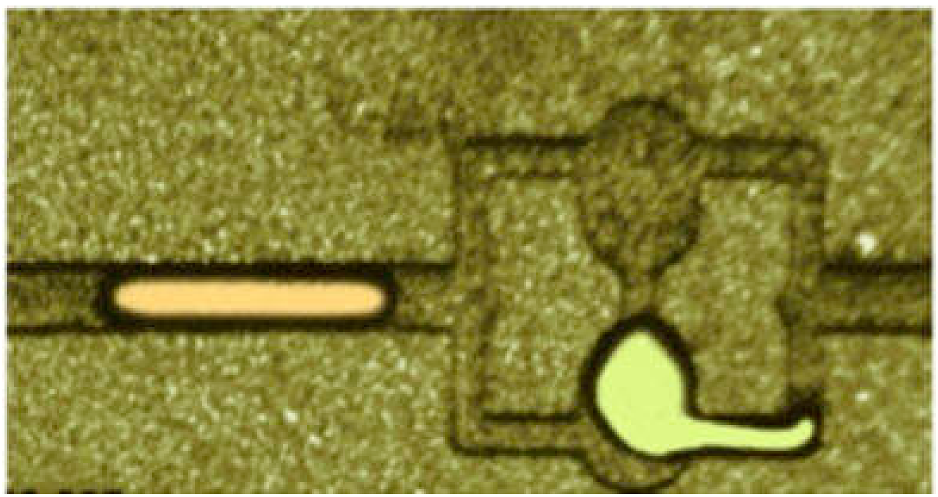

BISTABILITY

NONLINEARITY

AND/OR gate

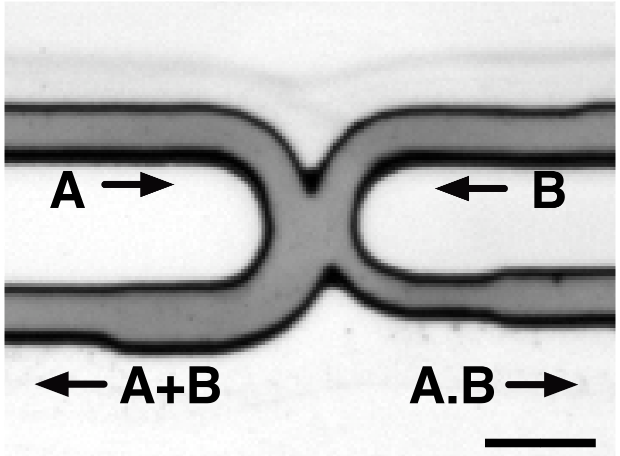

NOT gate

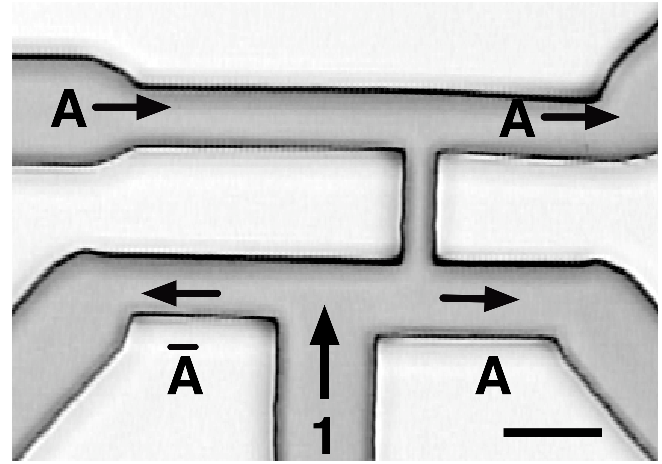

GAIN

INVERSION

BISTABILITY

Toggle Flip-Flop

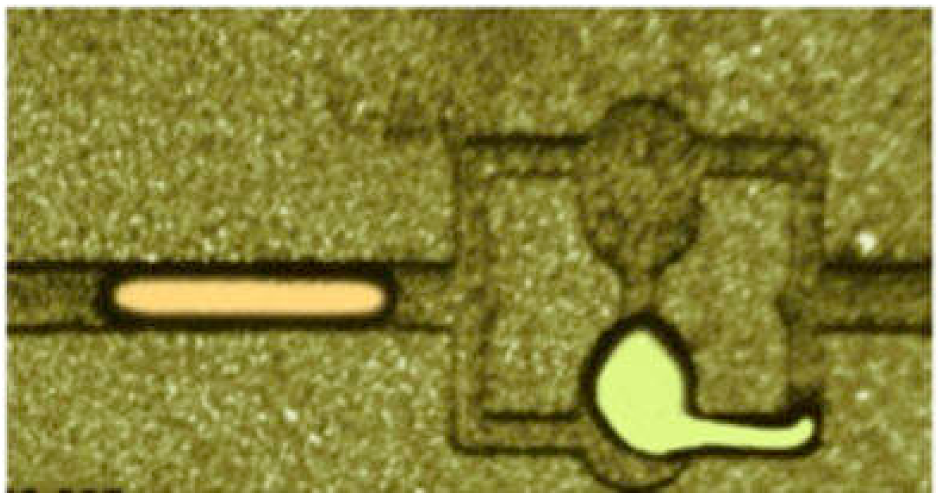

Ring Oscillator

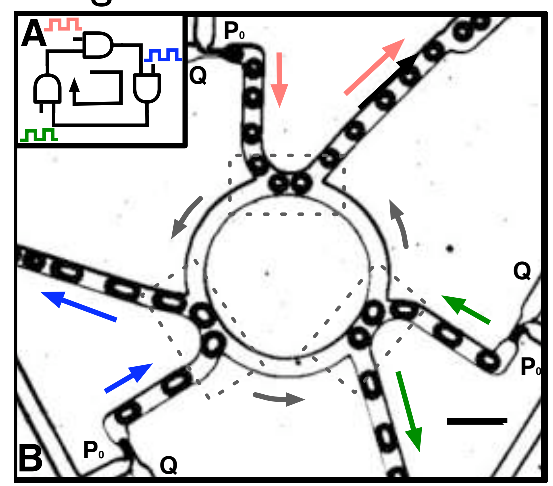

CASCADABILITY

FEEDBACK

NONLINEARITY

AND/OR gate

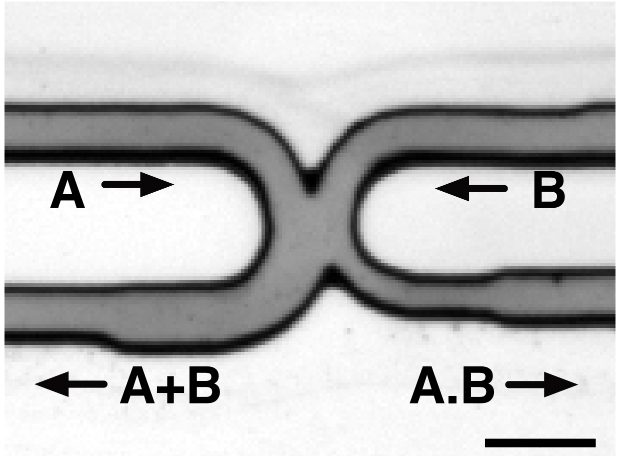

NOT gate

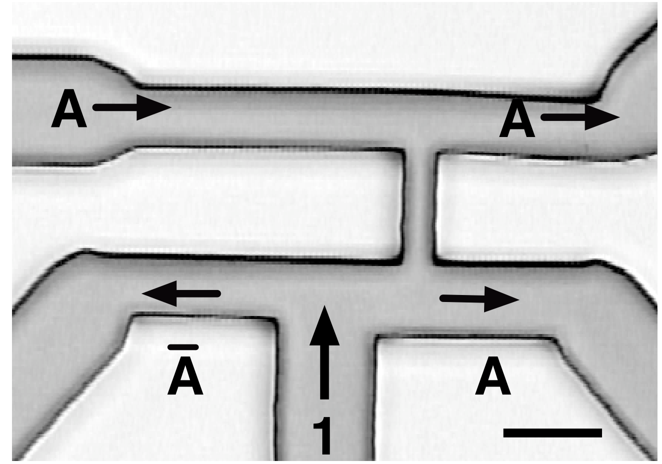

GAIN

INVERSION

BISTABILITY

Toggle Flip-Flop

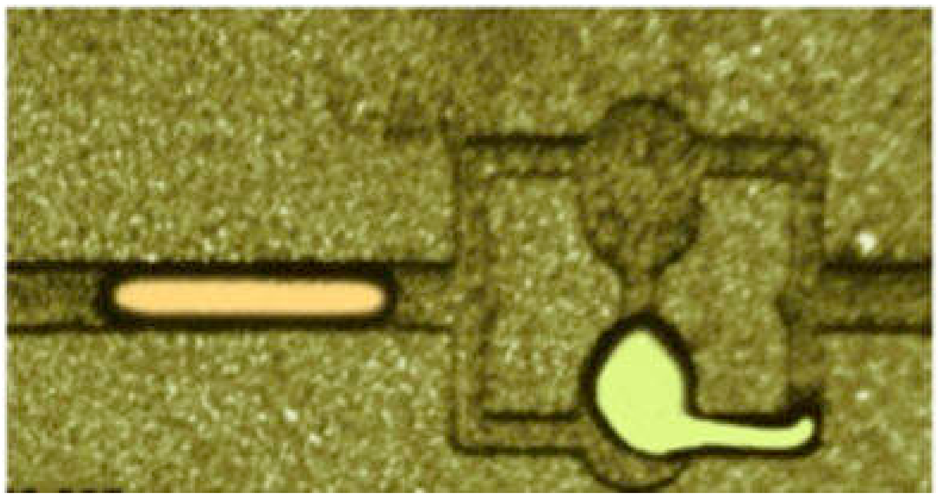

CASCADABILITY

FEEDBACK

Ring Oscillator

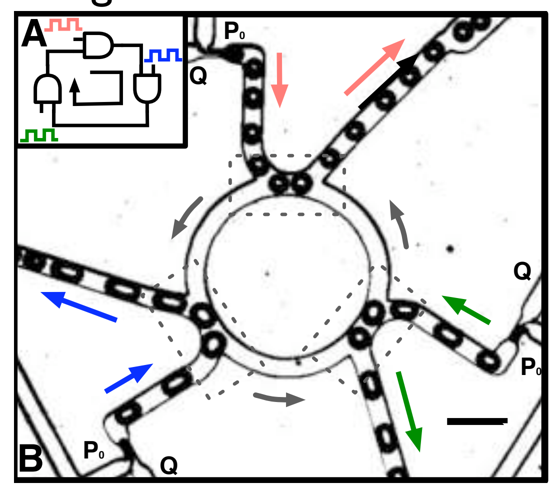

SYNC

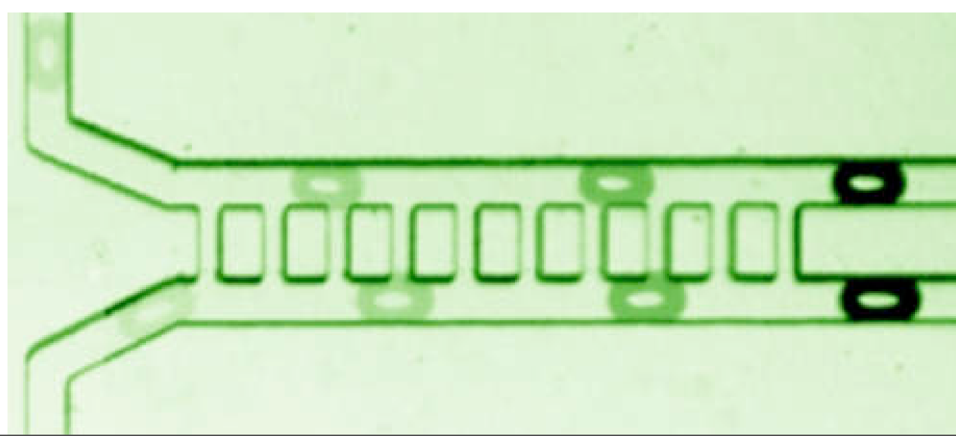

NONLINEARITY

AND/OR gate

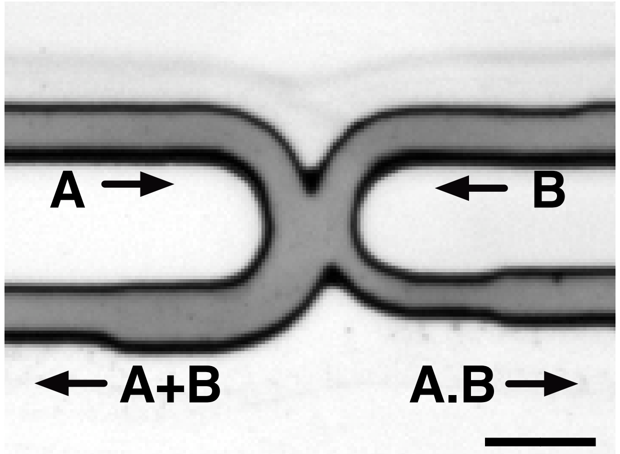

NOT gate

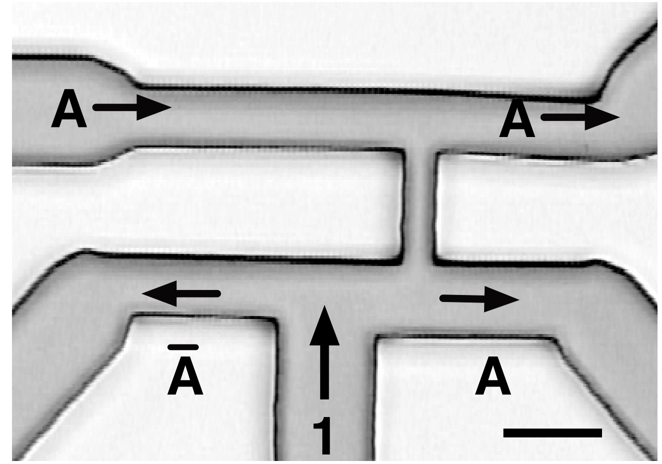

GAIN

INVERSION

BISTABILITY

Toggle Flip-Flop

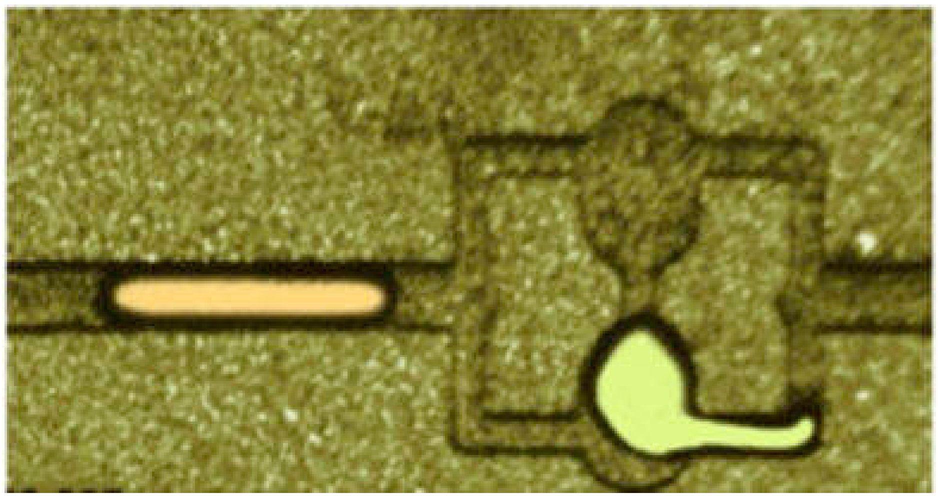

CASCADABILITY

FEEDBACK

Ring Oscillator

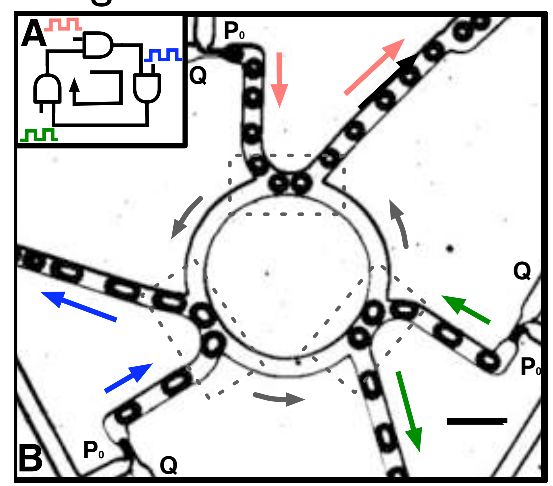

SYNC

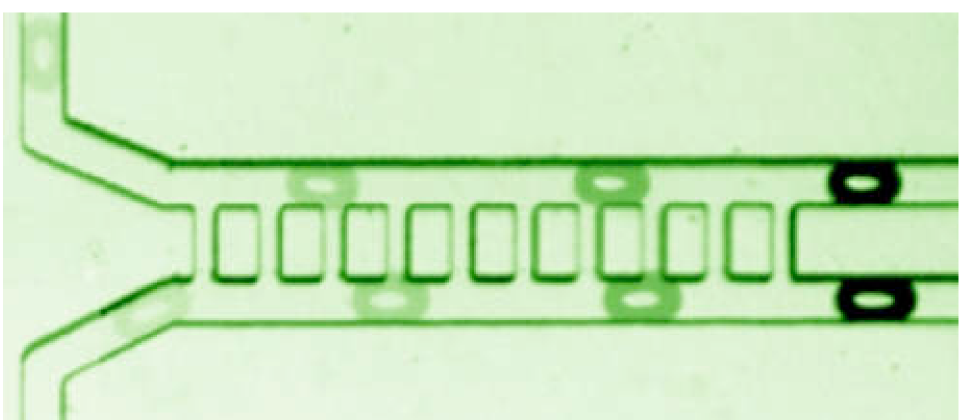

GEN.

Integration

Modular elements
Open source CAD
Component Libraries

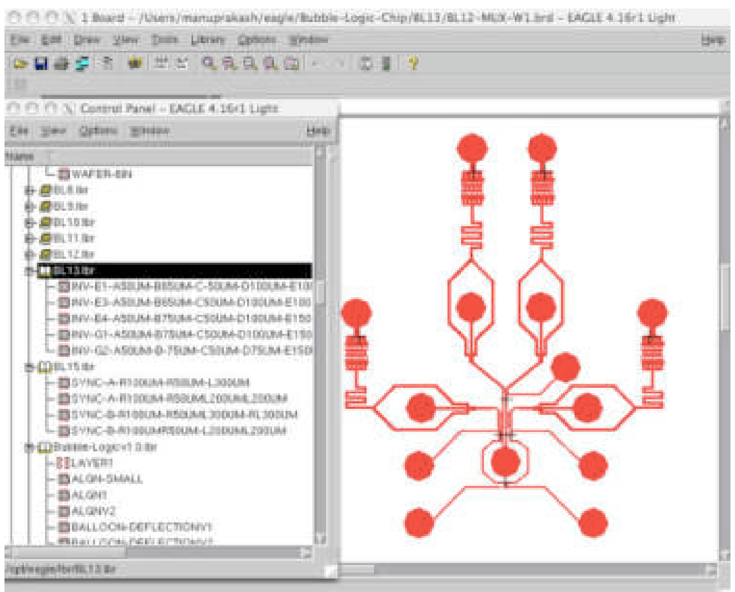

Random Access Chemical Memory

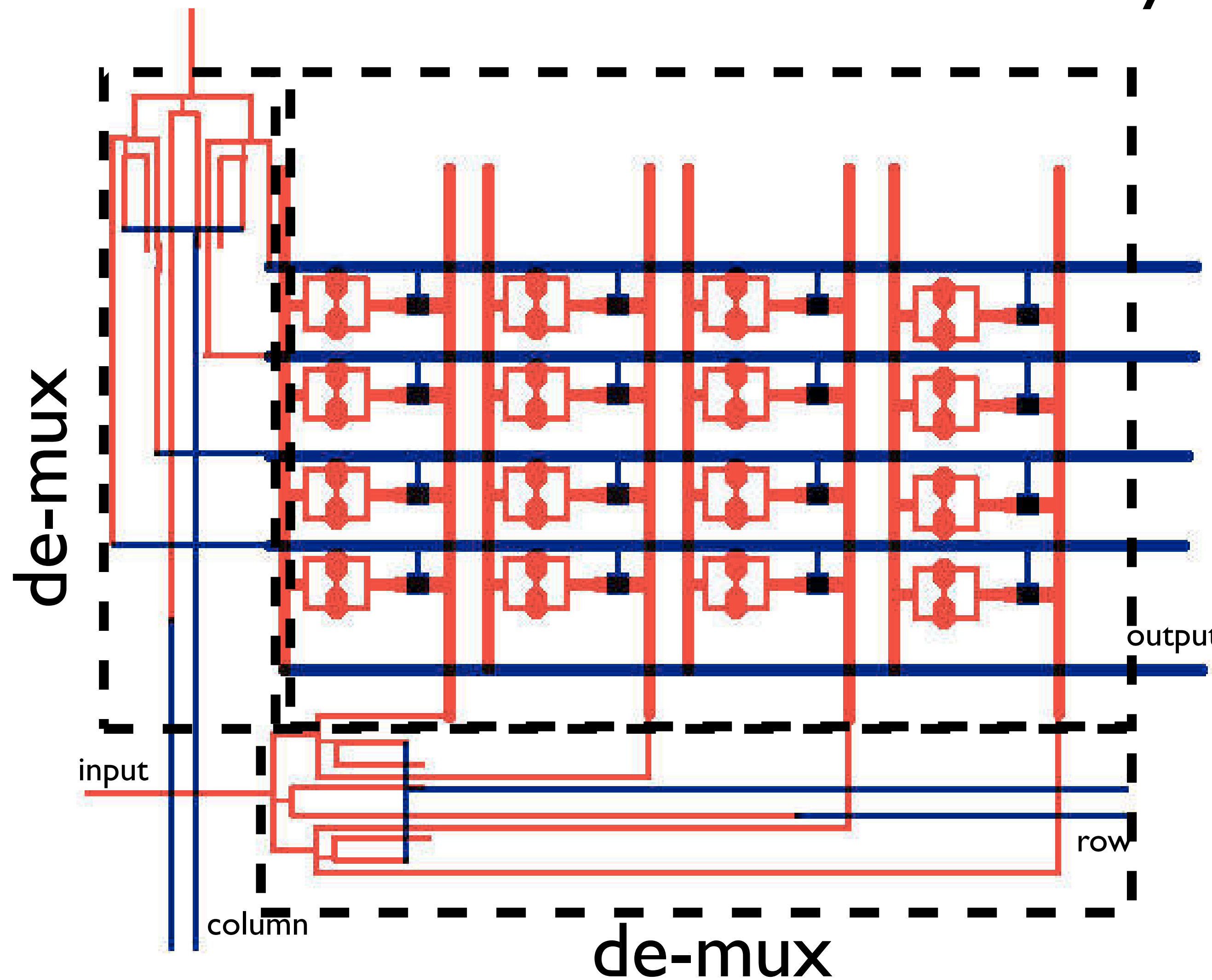

Self-clocked microfluidics?

Capillary Ratchets

Red-neck phalarope

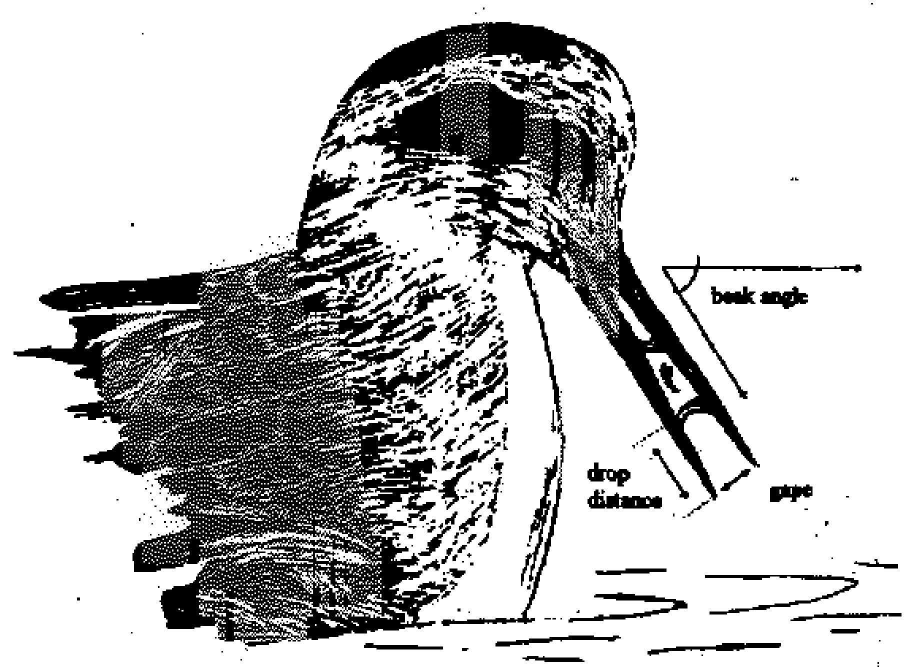

[Rubega et al, 93]

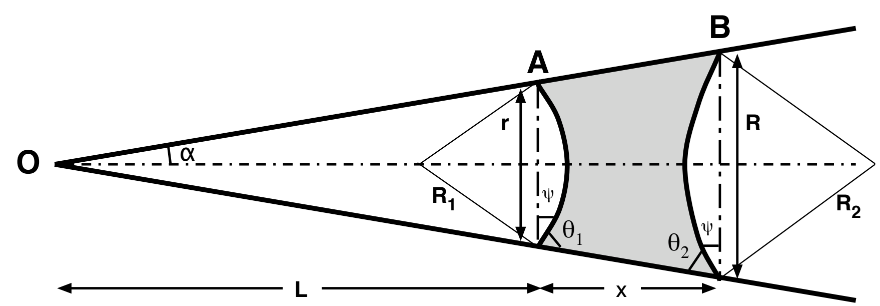

Capillary ratchet

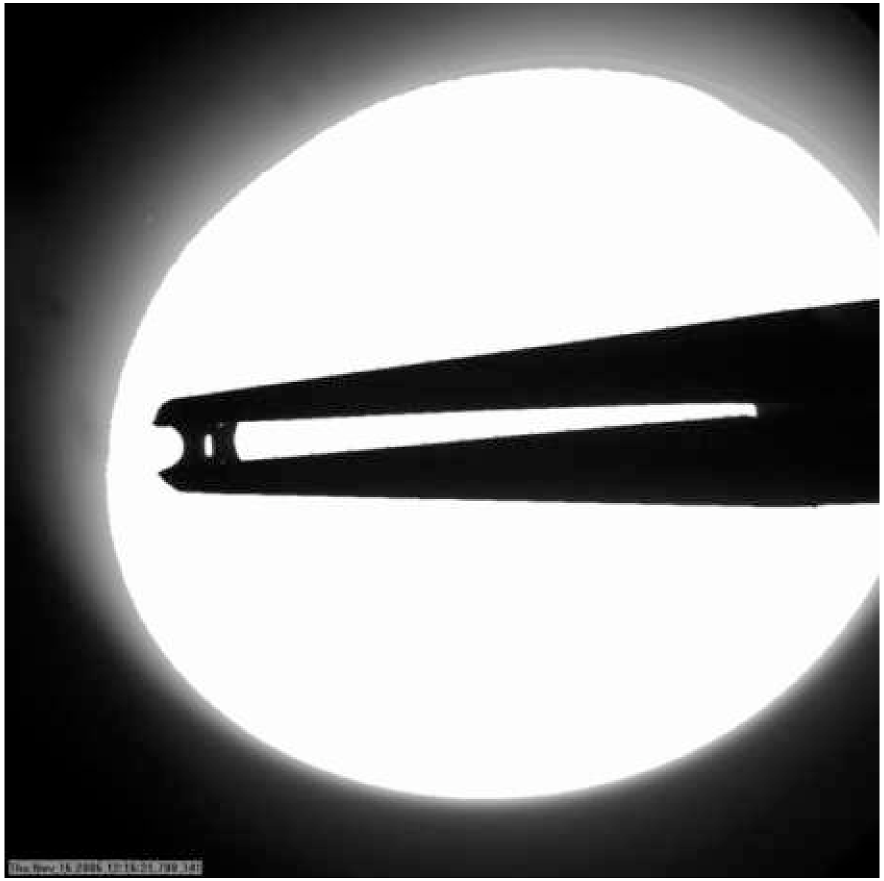

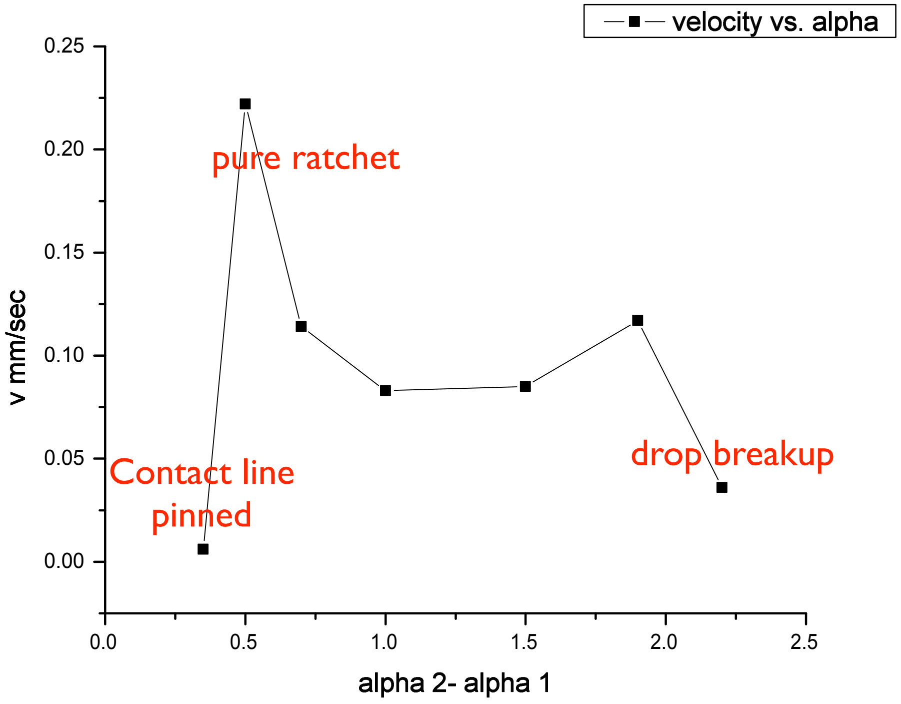

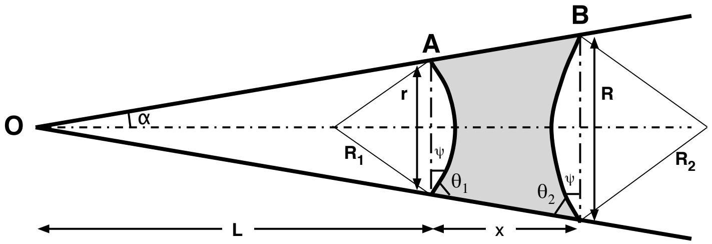

$$tan(\pi/4 - (\theta_a - \alpha_{min})/2) = \frac{3(x\alpha_{min}(x+2L) - 2V)}{4\alpha_{min}^2(L^2 + (L+x)^2}$$

$$tan(\pi/4 - (\theta_r + \alpha_{max})/2) = \frac{3(x\alpha_{max}(x+2L) - 2V)}{4\alpha_{max}^2(L^2 + (L+x)^2}$$

Can be solved graphically for alpha max and min
Criteria for alpha when the drop just starts to move

Line tension balance

$$\theta_1 - \theta_2 = 2\alpha$$

$$d\theta_1 - d\theta_2 = 2d\alpha$$

[Prakash et al. 2007 in prepration]

Ultra-Small-Sample Molecular Structure Detection Using Microslot Nuclear Spin Resonance

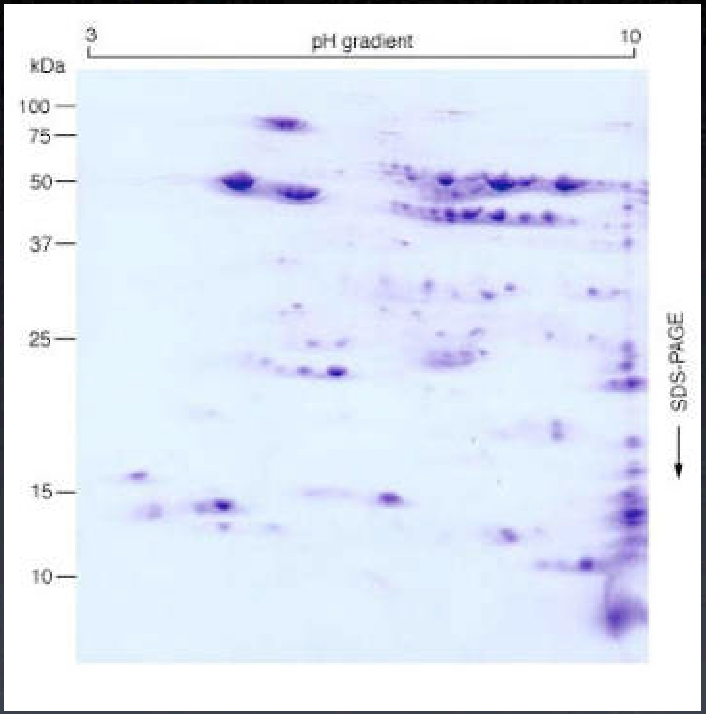

Yael Maguire

- To create a technology that can get structural information from 10^{13}-10^{14} (100pmols -1nmol) biomolecules and avoid DNA/bacteria amplification.

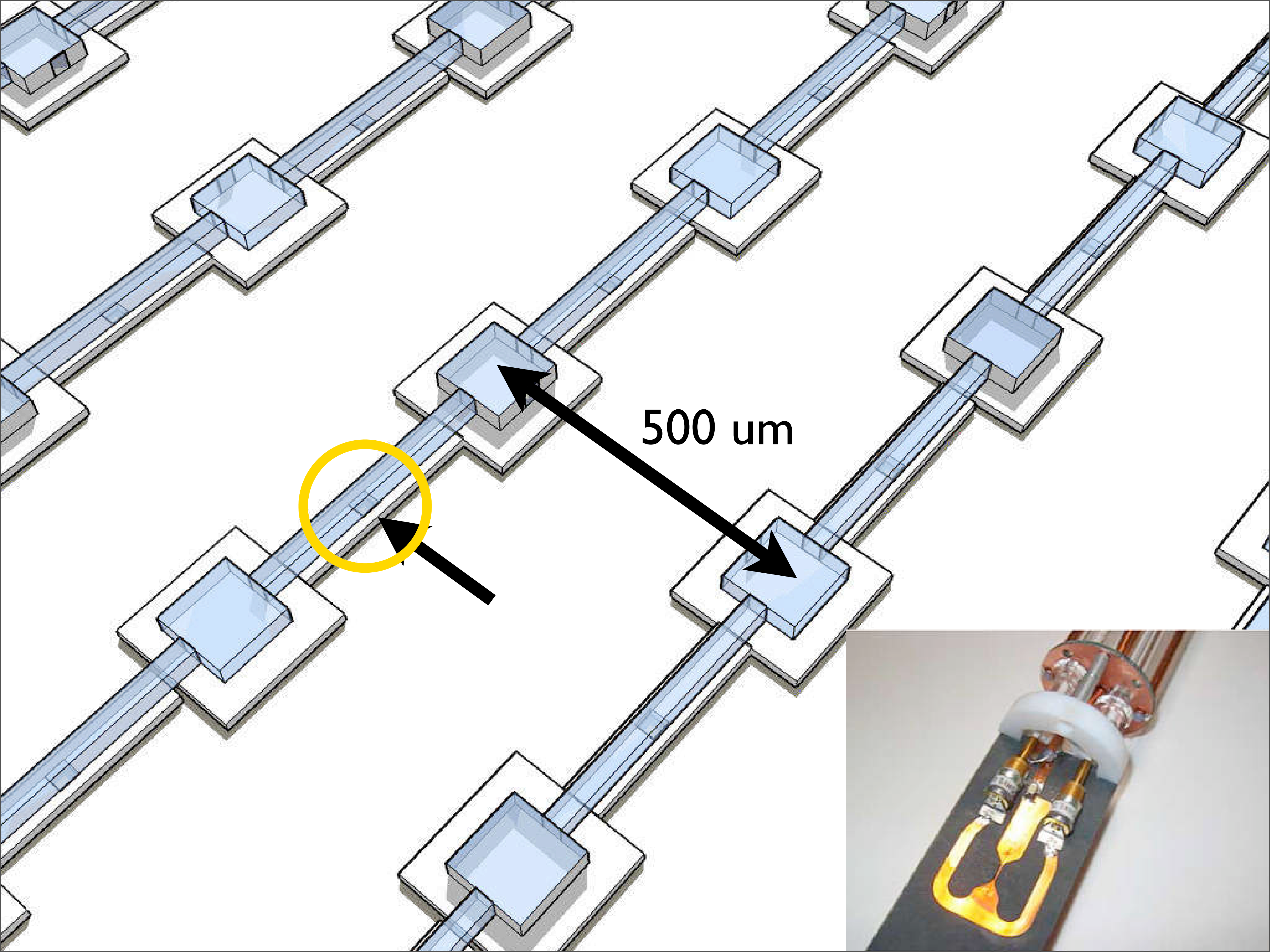
500 um

- highest SNR for planar detector
- demonstrated detection of ~ 10^{14} biomolecules
- scalable, parallel geometry to improve SNR_{puv}

Maguire et al, PNAS v104, n22 (2007)

Ultra-small-sample molecular structure detection using microslot waveguide nuclear spin resonance

Yael Maguire*†, Isaac L. Chuang*, Shuguang Zhang*†‡, and Neil Gershenfeld*

*Center for Bits and Atoms and ‡Center for Biomedical Engineering, NE47-379, Massachusetts Institute of Technology, Cambridge, MA 02139-4307

Communicated by Alexander Rich, Massachusetts Institute of Technology, Cambridge, MA, April 6, 2007 (received for review August 25, 2006)

We here report on the design of a planar microslot waveguide NMR probe with an induction element that can be fabricated at scales from centimeters to nanometers to allow analysis of biomolecules at nano- or picomole quantities, reducing the required amount of materials by several orders of magnitude. This device demonstrates the highest signal-to-noise ratio for a planar detector to date, measured by using the anomeric proton signal from a 15.6-nmol sample of sucrose. This probe had a linewidth of 1.1 Hz for pure water without susceptibility matching. Analysis of 1.57 nmol of ribonuclease-A shows high sensitivity in one- and two-

(RF) homogeneity (27). As with other miniaturized probes, a microslot has much shorter tipping times for the same power input and very little radiation damping compared with conventional probes, enabling more complex pulse sequences. Moreover, it is not only easily fabricated at a wide variety of scales, but multiple samples can be measured in parallel by an array. In realizing this design, we demonstrate the fabrication of this device and perform a set of experiments to determine the linewidth of water, measure the device's SNR, perform multiple-quantum measurements on a protein ribonuclease-A, and mea-

.4 m

~1 m

~4 m

Conclusions

Internal control scheme
Material independent
KHz operation
Digital control

Combinatorial chemistry
Chemical synthesis
High throughput screening
Large scale chemical memories
Handheld diagnostics

Printing
Physical Cryptography

Playground for fluid mechanicians